

**PREPARATION OF BIOMINERAL FILLER AND ITS  
APPLICATION AS BIOPOLYMER COMPOSITE FILLER**

**NUR DAMIA BT MOHD ISMAIL**

**FACULTY OF ENGINEERING  
UNIVERSITY OF MALAYA  
KUALA LUMPUR**

**2013**

**PREPARATION OF BIOMINERAL FILLER AND ITS APPLICATION AS  
BIOPOLYMER COMPOSITE FILLER**

**NUR DAMIA BT MOHD ISMAIL**

**RESEARCH REPORT SUBMITTED IN PARTIAL  
FULFILLMENT OF THE REQUIREMENT FOR THE  
DEGREE OF MASTER OF ENGINEERING**

**FACULTY OF ENGINEERING  
UNIVERSITY OF MALAYA  
KUALA LUMPUR**

**2013**

**UNIVERSITY OF MALAYA**

**ORIGINAL LITERARY WORK DECLARATION**

Name of Candidate: Nur Damia bt Mohd Ismail (I.C/Passport No:

Registration/Matric No: KGG110013

Name of Degree: Master of Engineering in Materials Engineering and Technology

Title of Research Report: Preparation of biomineral filler and its application as biopolymer composite filler

Field of Study: Polymer composite

I do solemnly and sincerely declare that:

- (1) I am the sole author/writer of this Work;
- (2) This Work is original;
- (3) Any use of any work in which copyright exists was done by way of fair dealing and for permitted purposes and any excerpt or extract from, or reference to or reproduction of any copyright work has been disclosed expressly and sufficiently and the title of the Work and its authorship have been acknowledged in this Work;
- (4) I do not have any actual knowledge nor do I ought reasonably to know that the making of this work constitutes an infringement of any copyright work;
- (5) I hereby assign all and every rights in the copyright to this Work to the University of Malaya ("UM"), who henceforth shall be owner of the copyright in this Work and that any reproduction or use in any form or by any means whatsoever is prohibited without the written consent of UM having been first had and obtained;
- (6) I am fully aware that if in the course of making this Work I have infringed any copyright whether intentionally or otherwise, I may be subject to legal action or any other action as may be determined by UM.

Candidate's Signature

Date

Subscribed and solemnly declared before,

Witness's Signature

Date

Name:

Designation:

## ABSTRACT

*Lokan* shell powder (LP), which is the source of biomineral Calcium Carbonate ( $\text{CaCO}_3$ ) has been incorporated into a biopolymer, PLA to produce thin film biocomposites. The incorporation of LP has been affecting the mechanical properties, crystallization and porosity of the PLA matrix. With the addition of LP, the stiffness of the composite was found to be increase significantly. In term of crystallization, the percentage of crystallinity decrease with the addition of LP and show significant drop at 8wt% filler content. FESEM result clearly showed the decrease in size and number of pores when LP is added to PLA matrix.

## **ABSTRAK**

Serbuk dari cengkerang Lokan yang merupakan sumber biomineral Kalsium Karbonat telah dicampurkan bersama dengan Asid Polilaktik, iaitu sumber biopolimer untuk menghasilkan komposit filem nipis. Campuran tersebut memberi perubahan kepada sifat mekanikal, pengkristalan dan juga keliangan matriks PLA. Jumlah Kalsium Karbonat juga mempengaruhi penambahan sifat kekakuan komposit dengan ketara. Dari segi pengkristalan, peratus kristal juga berkurang dengan setiap penambahan serbuk Lokan dan peratus Kristal didapati paling minimum dengan penambahan 8wt% kalsium karbonat. FESEM pula menunjukkan penambahan serbuk lokan mampu mengurangkan penurunan saiz dan bilangan liang pada matriks PLA.

## ACKNOWLEDGEMENTS

My greatest gratitude to Almighty God for given me blessing and opportunity in completing my research report. I would like to thank those who have given me priceless assistance in the completion of my Master of Engineering research project.

Upon completion of this project, I would like to express my deep and sincere gratitude to my supervisor, Dr. Amalina Muhammad Afifi, senior lecturer of the Department of Mechanical, University of Malaya. Her wide knowledge and ideas have been a great value for me. Her understanding, encouraging and personal guidance have provided a good basis for the present thesis. Also for her constructive comments and support throughout this work.

I also would like to thank Encik Aziz, Encik Zaharudin, Encik Syed, Encik Zaman and Encik Radzi from the Faculty of Engineering and Faculty of Science for their assistance during the characterization stage of my sample.

During this work I have collaborated with many colleagues for whom I have great regard, and I wish to extend my warmest thanks to those who had chipped in fragments of assistance to the completion of my project.

I owe my loving thanks to my parent Mohd Ismail and Raja Zahura. Without their encouragement and understanding it would have been impossible for me to finish this work. Also, my special gratitude to my brother, my sisters and their families for their loving support.

Nur Damia Ismail

## TABLES OF CONTENTS

	Page
<b>ABSTRACT</b>	iii
<b>ABSTRAK</b>	iv
<b>ACKNOWLEDGEMENTS</b>	v
<b>TABLE OF CONTENTS</b>	vi
<b>LIST OF TABLES</b>	ix
<b>LIST OF FIGURES</b>	viii
<b>LIST OF ABBREVIATIONS</b>	xi
 <b>CHAPTER 1 INTRODUCTION</b>	 1
1.1 Background	1
1.2 Problem statement	4
1.3 Significance of study	5
1.4 Objective of study	6
 <b>CHAPTER 2 LITERATURE REVIEW</b>	 7
2.1 <i>Polymesoda expanda</i> , Lokan	7
2.2 PLA	14
2.2.1 PLA polymerization routes	15
2.2.1.1 By step-growth polymerization of lactic acid with other hydroxyl acids	15
2.2.1.1 By chain-growth polymerization of the dimmer lactide	15
2.3 Role of PLA as matrix, CaCO <sub>3</sub> as filler in composite	18
2.3.1 Tensile properties	19
2.3.2 Crystalline properties of the composite	20
 <b>CHAPTER 3 METHODOLOGY</b>	 21
3.1 Materials	21
3.2 Instruments	21
3.3 Methods	23
3.3.1 Preparation of <i>Lokan</i> Powder (LP) Particle	23
3.3.1 Preparation of PLA polymer solution	23
3.3.1 Production of Thin Film composite	23
3.3.1 Scanning Electrone Microscope	24
3.3.1 Field Emmision Scanning Electron Microscope	24
3.3.1 Tensile testing	25
3.3.1 X-Ray Diffraction Analysis (XRD)	25
3.3.1 Differential Scanning Calorimeter (DSC) Analysis	26
 <b>CHAPTER 4 RESULT AND DISCUSSION</b>	 27
4.1 Characterization of Lokan Shell Powder	27
4.1.1 Identification of type of polymorph by XRD analysis	27
4.1.2 Surface morphology by SEM	28
4.1.3 Elemental analysis by EDX	31
4.1.4 Comparison of polymorph from different species of bivalves	33

4.2	Characterization of PLA/LP composite	35
4.2.1	X-Ray Diffraction Analysis	35
4.2.2	Crystallization behaviour surface morphology by SEM	38
4.2.3	Tensile properties	43
4.1.4	Surface morphologies of PLA/LP composite	50
 <b>CHAPTER 5 CONCLUSION AND RECCOMENDATION</b>		
5.0	Conclusion	56
5.1	Recommendation	58
 <b>CITED REFERENCES</b>		59
 <b>APPENDIX</b>		62

## LIST OF TABLES

<b>Tables</b>	<b>Description</b>	<b>Page</b>
<b>Table 2.1</b>	Checklist and distribution of edible species from eight different divisions in Sarawak, Malaysia.	9
<b>Table 2.2</b>	Habitat and morphological characteristics of Polymesoda spp found in Sarawak.	10
<b>Table 2.3.</b>	Physical properties of PLA (98% L-lactide), PLA (94% L-lactide) , PS and PET	17
<b>Table 4.1</b>	Elemental content of powder derived from of Lokan shell	32
<b>Table 4.2</b>	Polymorph of different species of bivalves shell.	34
<b>Table 4.3</b>	Summary of result from DSC analysis for all sample.	38
<b>Table 4.4</b>	Summary of Tensile Result	44

## LIST OF FIGURES

<b>Figures</b>	<b>Description</b>	<b>Page</b>
<b>Figure 1.1</b>	Internal and external view of <i>Polymesoda Expansa</i> ( <i>Lokan</i> shell)	4
<b>Figure 2.1</b>	Main features of a bivalve shell	8
<b>Figure 2.2</b>	Bivalve shell layer morphology	13
<b>Figure 2.3</b>	Chemical structure of L-lactic acid, D-lactic acid and polylactic acid (PLA)	14
<b>Figure 2.4</b>	Chemical Structure of LL-, meso- and DD-lactides	16
<b>Figure 2.5</b>	Relation between onset temperature, crystallization temperature, degree of crystallinity with nano $\text{CaCO}_3$ weight fraction	20
<b>Figure 4.1</b>	XRD patterns of the <i>Lokan</i> shell powder.	27
<b>Figure 4.2</b>	The surface morphology of the <i>Lokan</i> shell powder	28
<b>Figure 4.3</b>	The surface morphology of the inner and outmost surface	29
<b>Figure 4.4</b>	Cross-sectional area	30
<b>Figure 4.5</b>	Ventral part of the outmost surface	30
<b>Figure 4.6</b>	Dorsal part at the outmost surface	30
<b>Figure 4.7</b>	Yellow colour area of the dorsal part at the inner surface	31
<b>Figure 4.8</b>	White colour area of the dorsal part at the inner surface of the <i>Lokan</i> shell.	31
<b>Figure 4.9</b>	XRD pattern of neat PLA	35
<b>Figure 4.10</b>	XRD pattern of PLA/LP composite with 2wt% filler content	35
<b>Figure 4.11</b>	XRD pattern of PLA/LP composite with 6 wt% filler content	36
<b>Figure 4.12</b>	XRD pattern of PLA/LP composite with 10 wt% filler content	36
<b>Figure 4.13</b>	Crystallization onset temperature vs. filler content	39

<b>Figure 4.14</b>	Crystallization temperature vs. filler content	40
<b>Figure 4.15</b>	Degree of crystallization vs. filler content (wt%)	41
<b>Figure 4.16</b>	Enthalphy of fusion (J/g) vs. filler content ( wt%)	42
<b>Figure 4.17</b>	Relationship between elongation at break and filler content	44
<b>Figure 4.18</b>	Neat PLA and PLA/10wt% LP sample after fracture	45
<b>Figure 4.19</b>	Relationship between Young's Modulus and filler content	46
<b>Figure 4.20</b>	Relationship between tensile strength and filler content	46
<b>Figure 4.21</b>	Relationship between tensile energy absorption and filler content	47
<b>Figure 4.22</b>	FESEM of neat PLA	50
<b>Figure 4.23</b>	FESEM of PLA/2wt% LP	51
<b>Figure 4.24</b>	FESEM of PLA/4wt% LP	51
<b>Figure 4.25</b>	FESEM of PLA/6wt% LP	52
<b>Figure 4.26</b>	FESEM of PLA/8wt% LP	53
<b>Figure 4.27</b>	FESEM of PLA/10wt% LP	53
<b>Figure 4.28</b>	FESEM at Higher magnification of neat PLA and PLA/6wt% composite.	54

## LIST OF ABBREVIATIONS

LP	:	Lokan Powder
PLA	:	Polylactide acid
CaCO <sub>3</sub>	:	Calcium carbonate
SEM	:	Scanning Electron Microscope
FESEM	:	Field Emission Scanning Electron Microscope
DSC	:	Differential Scanning Calorimeter
EDX	:	Energy Dispersive X-Ray Spectroscopy
XRD	:	X-ray diffraction

## CHAPTER 1

### INTRODUCTION

#### 1.1 Background and problem statement

Biomaterial which mainly consists of organic-inorganic materials exhibit a very unique microstructure with excellent biological and mechanical properties. Because of these unique properties of the biomaterial, it has attracted many researchers and industries to use it.

Calcium Carbonate ( $\text{CaCO}_3$ ) is the most abundant biomaterials in nature and has three types of polymorph such as calcite, aragonite and vaterite (Manoli and Dalas, 2000). It can be obtained in most seashell and eggshells. Its powder was applied in many industrial applications such as paper, inks, plastics and medicines (Xiang *et al.*, 2004). In composite production,  $\text{CaCO}_3$  is one of the widely used filler infused in the plastics matrix composite (Rothon, 2007). Commercial  $\text{CaCO}_3$  from limestone is in the form of calcite (Nurul Islam *et al.*, 2013). Calcite can also be found at the outer layer of the several bivalves (Luts *et al.*, 1960; S.Mann, 2001) such as Pterioidea and Mytiloida (Kennedy *et al.*, 1969; Taylor *et al.*, 1969). Natural aragonite is from biogenic origin and it is denser than calcite. The specific gravity of calcite is 2.71 and aragonite is 2.93 (Pokroy *et al.*, 2007). Due to its higher density and biocompatibility, aragonite can be a good candidate to produce scaffold to repair fractured bone (Stupp and Braun, 1997). Aragonite can also be created in the lab but the quantity is very low (Lee *et al.*, 2001). Vaterite is a metastable  $\text{CaCO}_3$  and has been detected at

the upper layer and at the surface of freshwater cultured pearls (Ma and Dai, 2001). Currently, calcium carbonate polymorph can be synthesised in the lab under controlled environment such as temperature (Chen and Xiang, 2009) and chemical solution (Hu and Deng, 2004).

The usage of  $\text{CaCO}_3$  derived from waste of local resources can possibly reduce the cost of particle reinforcement and hence reduce the cost of composites. In Malaysia, edible brackish water bivalves is at the highest rank of the major seafood production (54%) followed by shrimp (17.3%) and marine fish (6.3%) (FAO, 2011). Among edible bivalves is *Polymesoda expansa* from Corbiculidae family. It is originally from Bangladesh, Cambodia, India, Malaysia, Philippines, Thailand and Vietnam but it also exists at Myanmar (FAO, 2011).

The sample of *Polymesoda expansa* for this study was collected from Kota Samarahan, one of the divisions in Sarawak, Malaysia. It is distributed at the mangrove and muddy area in the maximum divisions of Sarawak, the biggest state (FAO, 2011). The shell is dark green, hard and thick, and sub-trigonal in shape with eroded umbo. *Polymesoda spp* provide cheap protein source for the people of Sarawak (FAO, 2011) and can grow up to 10 cm big (Do *et al.*, 2012). There has been no recorded document has been produced on the characterization of this clam shell. Most of the literatures reported on the utilization of the different molluscs including this species as biomonitor or indicator for heavy metal pollution at estuaries and coastal water (Hamli *et al.*, 2012; Poutiers, 1998). In Malaysia, most of the researches related with the mollusc were about cockle shells or *Anadara granosa* (Ng *et al.*, 2005), *Perna viridis* (Ong *et al.*,

2009) and razor clam (Kanaraju, 2008). The main objectives of this research are to determine the polymorph of the calcium carbonate from clam shell of *Polymesoda expansa* and to use it as filler in biopolymer composite.

Biopolymers are polymers that are either biological in origin or susceptible to digestion by micro organisms or can be chemically breakdown by the environment. Thus, due to the high cost of the petroleum-derived products and the environmental hazards, there is a growing effort on the development, research and the application of biopolymer. Biopolymer can be classified in four categories depending on the synthesis or the sources of the polymer (Vieira *et al.*, 2011).

a) Polymer from biomass such as the agro polymers from agro resources

i) Polysaccharides e.g starches from wheat potato and maizes, ligbo-cellulosic products ( straw,wood) and others ( chitosan, chitin)

ii) Protein and lipids,e.g animals ( collagen/gellatin)

b) Polymers obtained by microbial production, e.g polyhydroxyalkanoates (PHA) such as poly (hydroxybutyrate) (PHB)

c) Polymers that are chemically synthesized using monomers obtained from agro-resources, e.g poly (lactid acid) (PLA)

d) Polymers whose both monomers and polymers obtained by chemical synthesis from fossil resource, e.g polycaprolactones (PCL)

For this research, PLA has been chosen as biopolymer of interest. PLA is in the third category where it is a biodegradable polyester that is chemically synthesized from lactic acid or lactide which can be produced from renewable agro-resources such as sugarcane or corn. PLA has a good biodegradability and good process ability made it regarded as the most promising biodegradable polymer as was expected to substitute some of the non biodegradable engineering plastics.

## 1.2 Problem statement

It is reported that approximately 70 million tones of organic wastes are generated annually as municipal solid wastes, agricultural residues, animal wastes, sewage sludge from wastewater treatment plant, wood chips and even sea creature. Most of these wastes are either incinerated or dumped in landfill, both of which have serious impact on the environment. Therefore, Malaysia needs to adopt more practical, economical and acceptable approach in managing and disposing the organic wastes. One of the ways we can do this is by finding a useful function for waste from our daily lives instead of just throwing them away. Taking this into consideration, this study is dedicated to produce composites made from local waste product.

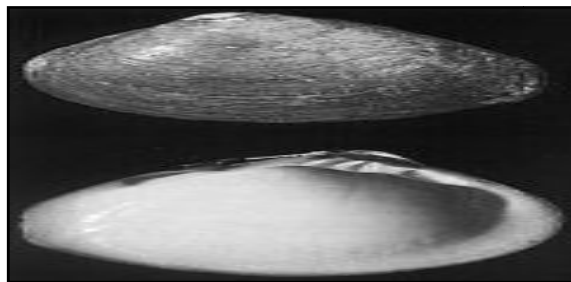


**Figure 1.1** Internal and external view of *Polymesoda Expansa* (Lokan shell)

A type of clam shell locally known as '*Lokan*' (shown in Figure 1.1) was chosen to be used in forming a composite material. "*Lokan*", or also known by its scientific name as *Polymesoda expansa* is a type of large clam that makes its habitat buried in the landward fringe of mangroves. Formerly, this large, heavy bivalve was known as *Genolia expansa*. It is well adapted to its habitat, being able to tolerate long periods of low tide and continue filter-feeding rapidly when inundated (Ng et al., 2005). Not much research has been done on the compositions of the "*Lokan*" shell. However, a research done on another close bivalve, the blood cockle shows that calcium carbonate,  $\text{CaCO}_3$  makes up about 98.7% of the total mineral composition of the shell (Hazmi et.al., 2007). According to another source, plants and animals absorb calcium carbonate from water - where it exists, in most cases, in the dissolved form of calcium hydrogen carbonate  $\text{Ca}(\text{HCO}_3)_2$  (Euro. Calcium Carbonate Association, 2004). From these statements, we can safely assume that the "*Lokan*" shell is also made up of a large portion of calcium carbonate.

### **1.3 Significant of studies**

The intention of this research is to study the effect of *Lokan* powder on the properties of *Lokan* powder/ polylactide thin film composites. As *Lokan* Powder is from biological source, which is also renewable resource, when it is incorporated with polylactide, a biopolymer, it will result in a better properties of biocomposites which can be used in bio-related application and also as good biodegradable composite to replace the conventional petroleum based polymer.

### 1.3 Objective of Study

The specific objectives of the project include;

1. To prepare *Lokan* powder and characterize its properties..
2. To study the effect of the incorporation of *Lokan* powder to the physical and mechanical properties of biopolymer Polylactide.
3. To examine the *Lokan* Powder particle distribution in PLA matrix.

## CHAPTER 2

### LITERATURE REVIEW

#### 2.1 *Polymesoda expansa* (*Lokan*)

*Polymesoda expansa* or locally known as *Lokan*, is one of the largest mangrove bivalve species distributed in the mangrove swamp. It can grow up to 10 cm diameter (Poutiers, 1998). Formerly, this large, heavy bivalve was known as *Genolia expansa* (Morton, 1984). It is originally from Cambodia, Malaysia (Peninsular Malaysia, Sarawak), Philippines, Thailand and Vietnam. However, currently it is widely distributed throughout West Indo-Pacific region ([www.iucnredlist.org](http://www.iucnredlist.org)) and also exists in Vanuatu, India and Sri Lanka (Morton, 1984). According to Poutiers (1998), *Polymesoda expansa* is in the group of Corbiculidae where it was first found in Mousson on 1849. The characteristics of Corbiculidae in general are shown in Figure 2.1. Figure 2.1 also shows how to measure shell height, length and width. Height is the distance from the bottom of the hinge of the shell to the top of the shell. Length is the widest part across the shell at 90 degrees to the height whereas width or hinge width (inflation) is measured at the thickest part.

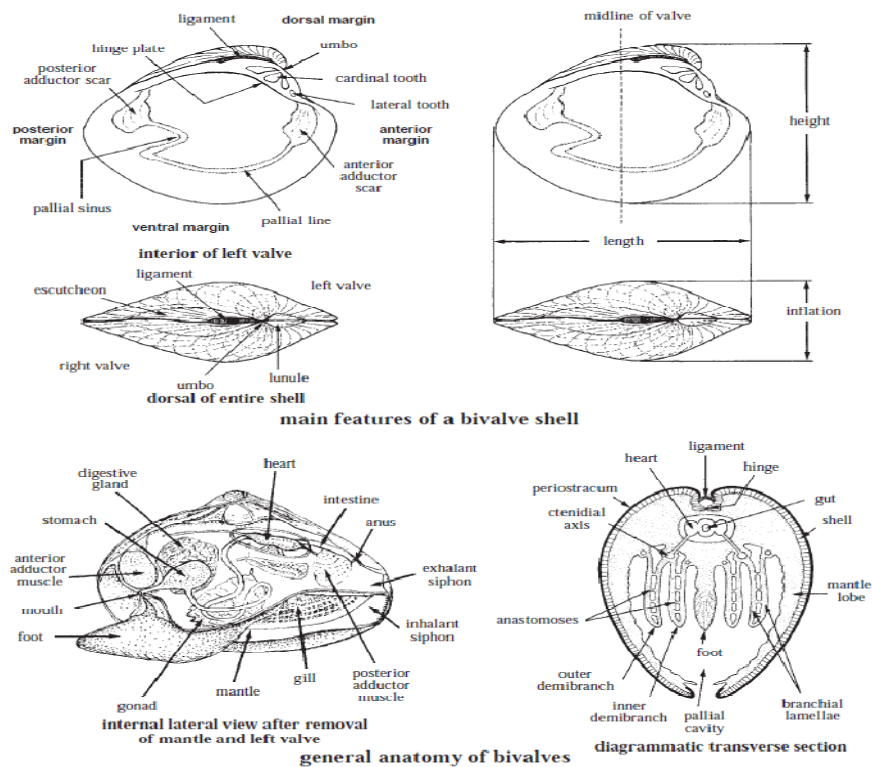


**Figure 2.1** Main features of a bivalve shell (Poutiers, 1998)

Bivalves including *Polymesoda expansa* are extraordinary organism where they can adapt successfully in the extreme environment in mangrove by changing their behaviour and physiological features (Pechenik, 2000), such as closing their hard shell to prevent dehydration. *Polymesoda expansa* is well adapted to its habitat, being able to tolerate long periods of low tide and continue filter-feeding rapidly when inundated (Ng and Sivasothi, 2005). It was reported that this species is currently not listed as a threaten species ([www.iucnredlist.org](http://www.iucnredlist.org)). However, any activities related to the destruction of the mangrove area may affect its existence in future. In addition, low pH value also can be detrimental to any molluscs species because acidic environmental may cause erosion to their external shell (Plaziat, 1984).

Hamli *et al.* ( 2012), conducted a study of the distribution of edible bivalve in eight divisions of Sarawak . However, Kota Samarahan division was not in the list of their study. The study found that the diversity of edible bivalves was found highest in Kuching and Bintulu compared to other six divisions. Generally in Sarawak, a large number of bivalves provide an essential part of protein in the diet of local community and some species add an important role in fishery economy of the state. Table 2.1 shows the distribution of *Polymesoda spp* in eight selected divisions from the study done by Hamdi *et al.*,( 2012). Some researchers stated that *Polymesoda expansa* also exist in Asajaya, Kota Samarahan (Kunding, 2009). Table 2.2 shows the habitat and the morphological characteristics of *Polymesoda spp*.

**Table 2.1** Checklist and distribution of edible species from eight different divisions in Sarawak, Malaysia. (Hamli et al,2012)

Family	Species	Kuching	Sarikei	Sibu	Mukah	Bintulu	Miri	Limbang	Lawas
Corbiculidae	<i>Polymesoda bengalensis</i>	+	+	+	-	+	+	+	-
	<i>Polymesoda erosa</i>	-	-	+	+	+	+	+	+
	<i>Polymesoda expansa</i>	-	-	-	-	+	+	+	+

(+)=present, (-)=absent

**Table 2.2** Habitat and morphological characteristics of *Polymesoda* spp found in Sarawak. (Hamli *et al.*, 2012)

Species	Lokal Name	Habitat	Characteristic
<i>Polymesoda bengalensis</i>	Lokan bakau	Brackish water	Hard and thick sub-trigonal, eroded umbo, dark green
<i>Polymesoda erosa</i>	Lokan apung	Brackish water	Hard and thick sub-rhomboidal, eroded umbo, green
<i>Polymesoda expansa</i>	Lokan selam	Brackish water	Hard and thick, trigonal ovate, eroded umbo, yellow

Not much research has been done on the compositions of the *Lokan* shell and its usage. Most of the literatures reported on the utilization of different types of molluscs to determine the concentration of heavy metals in the water because they tend to accumulate metals in their body tissue. Heavy metal contamination may retain in the water body and taken up by plankton, mollusc, and fish before transferred to human through food consumptions. Mollusk such as clams, mussels, cockle and oyster are widely reported in literature as biomonitors or indicator for heavy metal pollution at estuaries and coastal water due to their abundance, sedentary, easily collected, weighed (Yap and Cheng, 2006). Muhamad Yusoff and Mohd Long (2011) used *Lokan* as one of the molluscs to

assess environmental contamination especially to determine the concentration of heavy metals such as Cd, Cr, Cu, Zn and Mn at the estuary of Sungai Sematan. They found that *Lokan* was able to accumulate the highest amount of Cd, Zn and Mn compared to other molluscs such as *Meretrix meretrix*, *Nerita lineate*, *Cerithidea obtuse*, and *Crassostrea virginica*. Musa *et al.* (2008) examined the component of vibrio spp in bacteria and microflora of wild growing *Polymesoda expansa*. They found that *Polymesoda expansa* has been the carrier of some of *Vibrio spp.* such as *V. parahaemolyticus*, *V. alginolyticus*, *V. fluvialis* and *V. harveyi*. Consumption of seafood contaminated with *Vibrio spp.* may be dangerous to those with weak or impaired immune system and also could pose food poisoning to consumer if they are taking undercooked clam.

The mollusc shell has several functions. Its main functions are as a skeleton for the attachment of muscles, and to support and protect the clam inside the shell against predators. The mangrove area generally exposed to the changes of physiochemical characteristics such as salinity, dissolved oxygen content, pH and temperature, due to tidal fluctuation (Pechenik, 2000). In order to survive in harsh condition, bivalves have developed an outer layer or shell to protect them from dehydration during the low tide, attacked by predators and high temperature (Hashim, 1993). According to Lent (1969), bivalves can survived for a long periods of exposure as long as they were protected from desiccation (Pechenik,2000). The presence of concentric rings on the bivalve external shell surface has been extensively used to age them. The rings have been shown to be annual in origin and thus can be used as a reliable estimate of age (Gosling, 2003). The ring also can be found at the inner nacreous layer shell. The

formations of the rings in the inner nacreous layer are formed at a rate of one per year during spring (Lutz, 1976) and can be clearly seen under microscope.

The main component of the mollusc shell is calcium carbonate. Calcium is obtained from the diet or taken up from seawater. Carbonate is derived from CO<sub>2</sub>/bicarbonate pool in the animal's tissue. Then calcium carbonate is formed by the deposition of crystals of the salt in an organic matrix of the protein called conchiolin. The shells of bivalves are made of three layers (Gosling, 2003). The three layers are an outer periostracum, a middle prismatic layer and inner calcareous layer.

- i) Periostracum layer: A thin outer layer consists of horny conchiolin. It is often much reduced due to mechanical abrasion, fouling organisms, parasites or disease
- ii) Prismatic layer: It consists of aragonite or calcite, a crystalline form of calcium carbonate
- iii) Nacreous layer: It can be either a dull texture or iridescent mother-of-pearl, depending on the species. The surface is smooth to provide comfortable space for the clam inside.

Wilbur (1961) mentioned that the calcareous shells of bivalves are multilayered and consist of two intermixed phases. They are an organic matrix and crystalline calcium carbonate in the form of calcite or aragonite. Majority of the bivalve shells have different layers composed of calcite and aragonite. However, some bivalves may consist of more calcite than aragonite such as oyster. Some may

have entirely aragonite. Those phases may exist in a number of recurrent patterns, occurring in the discrete shell layers. Six types have been differentiated and are shown in Figure 2.2.

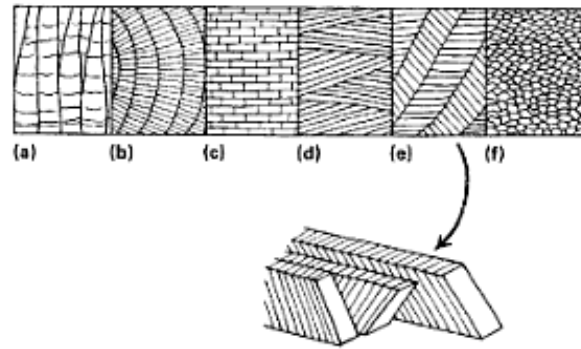


**Figure 2.2** Bivalve shell layer morphology as seen in thin section: (a) a simple prismatic (b) compound prismatic (c) sheet nacreous (d) foliated (e) crossed lamellar with inset showing disposition of stacked aragonite lamellae (f) homogeneous (Taylor and Layman, 1972)

The followings are brief explanation on the six types of patterns that may exist in the shell layers (Taylor *et al.*, 1969)

- (i) Simple prismatic structure with columnar polygonal calcite or aragonite prisms
- (ii) Composite prismatic structure with tiny radiating acicular crystals
- (iii) Nacreous structure in which tabular sheets of aragonite are found resembling a brick wall when cut in section. These are usually found in middle and inner shell layers
- (iv) Foliated structure of lath-like calcitic crystallites arranged in sheets

- (v) Cross-lamellar structure which is normally aragonitic. Here the shell is made of closely spaced lamellae, within each of which are found thin stacked plates of aragonite, those of adjacent lamellae being inclined in opposite directions to one another. In some cases intergrowth of blocks of crystals are found (complex crossed-lamellar structure) with four principal orientations.
- (vi) Homogeneous structure with small granular anhydral crystals.

## 2.2 PLA

PLA consists of lactic acid as the basic constitutional unit. It is manufactured by carbohydrate formation or chemical synthesis (Auras et.al ; 2004). Lactic acid (2-hydroxy propionic acid) is a hydroxyl acid with an asymmetric carbon atom and exists in two optically active configurations, the L (+) and D(-) isomers. In general, lactic acid can be manufactured from petroleum based sources or from renewable source such as glucose and maltose from corn or potato, sucrose from cane or beat sugar etc. Chemical structure of PLA is shown in figure 2.3.

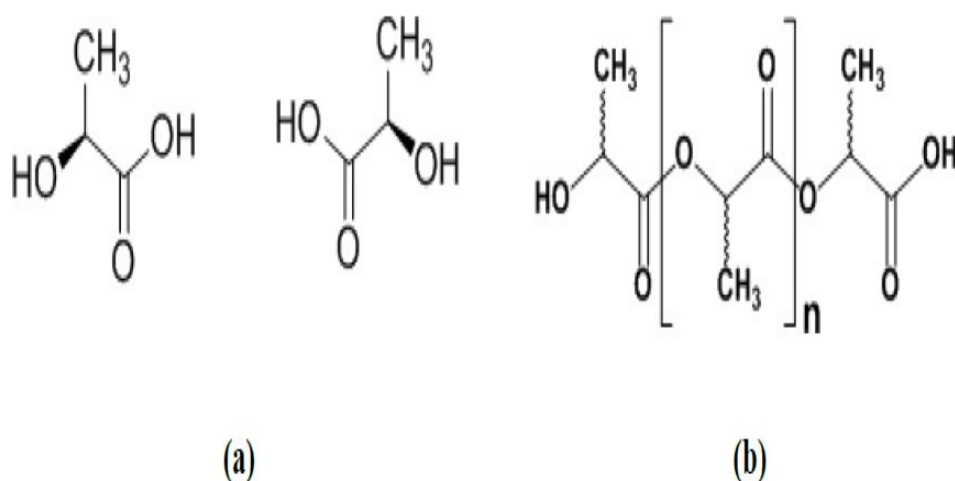


**Figure 2.3** Chemical structure of (a) L-lactic acid, D-lactic acid and (b) poly(lactic acid) (PLA)

In addition to its biodegradable character, other advantage of PLA polymer are biocompatibility, availability from renewable resource, non toxic by products, metabolization or mineralization of biodegradable byproducts and change to cover large range of properties through copolymerization or blending (Vert et al., 1995; Lunt, 1998).

### **2.2.1 PLA polymerization routes**

It is possible to produce lactic acid based polymers from various monomers via different routes.

#### **2.2.1.1 By step-growth polymerization of lactic acid with other hydroxyl acids**

This polymerization method (of mixtures of L- and D-lactic acid) reportedly leads to random distribution of the L and D units. Since the step growth polymerization is an equilibrium reaction, the presence of even trace amount of water in late stages of polymerization can limit the ability to form high molecular weight polymer. Other drawback of direct synthesis of PLA by polycondensation of lactic acid is high enough that high molecular weight can be achieved only above 99% conversion also monofunctional impurities such as ethanol or acetic acid from fermentation can limit the molecular weight. Due to these limitations, it is difficult to obtain high molecular weight polymer PLA (Drumright, 2000)

### 2.2.1.2 By chain-growth polymerization of the dimmer lactide

Three stereoisomer of lactic acid exists namely, i) L-lactide, ii) D-lactide and iii) meso-lactide . The stereochemical composition of the resulting polymer is therefore determined by the makeup of the lactide monomer stream. The three chemical structures are shown below in Figure 2.4

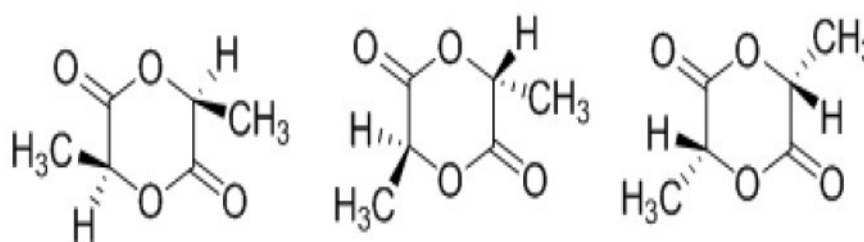


**Figure 2.4** Chemical Structure of LL-, meso- and DD-lactides

Lactide structure shown in Figure 2, is composed of two lactic acid units linked by two ester bonds to form dimeric cyclic monomer. The cyclic dimers bear two asymmetric carbon atoms. High molecular weight polymer can be obtained via ring opening polymerization of lactide containing feeds in organic solution or in the bulk at different temperatures. The chain growth polymerization can proceed by different mechanism, e.g., cationic, anionic etc. (Vert et al., 1995) has discussed the various polymerization routes of lactides, namely melt, bulk, suspension and solution polymerization in details.

Depending on the synthesis route and the chiral monomer(s) used, the resulting distribution of chiral repeating units can be very different. The use of cyclic dimer (lactide) together with control residence time, temperature and catalyst type used make it possible to control the ratio and sequencing of D- and L- lactic

acid units in the final polymer ( Lunt, 1998). The optical composition of the polymer significantly affects crystallization kinetics and the ultimate extent of crystallinity. PLA derived from greater than 93% L-or D-lactic acid can be semi crystalline whereas PLA containing greater than 7% of second isomer is found to be amorphous (Auras et al., 2004). This second isomer acts as an impurity leading to introduction of twists in the otherwise regular polymer molecular architecture. The molecular imperfections result in decrease in both the rate and extend of PLA crystallization. Ikada and Tsuji ( 2000) have reported that the glass transition temperature.  $T_g$  is determined by the proportion of different lactides present, which result in PLA polymers with wide range of stiffness and hardness value. Table 2.3 gives the physical properties of PLA (98% L-lactide), PLA (94% L-lactide), polystyrene (PS) and polyethylene terephthalate (PET).

**Table 2.3.** Physical properties of PLA (98% L-lactide), PLA ( 94% L-lactide), PS and PET ( David, 1994)

Sample	PLA (98% L-lactide)	PLA ( 94% L-lactide)	PS (atactic)	PET
$T_g(^{\circ}\text{C})$	71	66	100	80
$T_m(^{\circ}\text{C})$	160-170	140-150	-	240-245
Enthalphy of fusion (J/g)	37.5	21.9	-	47.7
% crystallinity	40	25	-	38

In spite of PLA having similar  $T_g$  and  $T_m$  values as those of commodity plastics like PS and PET, PLA has its own drawbacks. PLA can be degraded by the presence of residual metals or catalyst (Cam and Marucci, 1997). This residual metal can catalyze chain transfer, transesterification and depolymerization reactions. PLA is hydrolyzed by trace amounts of water and this reaction is further catalyzed by the hydrolyzed monomer (lactic acid) which may result in zipper-like depolymerization reactions. PLA chains can also undergo oxidative random chain scission and transesterification giving monomer and oligomeric ester (Celli and Scandola, 1992). Thermal history can induce changes in the crystallinity and thus affect the physical properties of PLLA. Properties such as tensile strength are reported to improve with increasing L-lactide content of the PLA sample (Perego et al., 1996). Annealing of PLLA increases the tensile and impact strength due to increase in crystallinity and the physical cross-linking effects of crystalline domains. The mechanical properties of PLA are comparable to those of commodity polymers like PS. However the main advantage of PLA over these and other widely used olefinic polymers is its ability to undergo degradation producing water and carbon dioxide. Properties of PLA can be tuned by controlling the stereochemical structure of the polymer, blending of PLA with other polymer, e.g. cellulose or by addition of particles, e.g. calcium carbonate particles to the PLA matrix.

All these observations afford us the possibility of preparing PLA composites with improved properties.

### **2.3 Role of PLA as matrix, CaCO<sub>3</sub> as filler in composite.**

Many research has been done to study the composite with PLA as matrix, CaCO<sub>3</sub> as filler, or the incorporation of the PLA and CaCO<sub>3</sub>. In current research, *Lokan* is the source of CaCO<sub>3</sub>.

#### **2.4.1 Tensile properties**

As CaCO<sub>3</sub> is the main concern of this research, the tensile properties of composite with CaCO<sub>3</sub> are further discussed. Jiang et.al, has study the tensile properties of PLLA/nano-sized Calcium Carbonate (NPCC) and from his study he found that the Yield strength decrease and Young Modulus increase with the addition of NPCC. Massive crazing also occurred in all composite samples. Massive crazing in the sample is due to the debonding of the particle surface. The relatively easy debonding in his sample is due stearic acid coating on the particle which limits the interaction between NPCC with PLLA. The cubic shaped of particle also is one the reason for the existence of debonding. The cubic shaped of particle cause high stress concentration around NPCC particle, thus promote debonding.

The incorporation of Calcium Carbonate in other type of matrix is also discussed by other researcher. Lam *et al.* has discussed the mechanical properties of Calcium Carbonate in Polypropylene Lam *et al.* has studied the mechanical properties of PP composite with untreated micron size Calcium Carbonate, untreated nano size Calcium Carbonate and stearic acid treated nano size Calcium Carbonate. The addition of Calcium Carbonate in PP, increased the Yield Strength, increased Modulus of Elasticity (MPa) and decreased the Elongation at break (%) comparing to neat PP. For Yield Strength and Modulus

of Elasticity, both value increased with the increased filler content until maximum value before it start to decrease. Treated nano size Calcium Carbonate give the best improvement of the composite tensile properties where maxima Yield Strength and Modulus of Elasticity were reached at 15wt%-20wt% filler content.

#### 2.4.2 Crystalline properties of the composites

It is generally believe that the crystallization behaviour is closely related to physical and mechanical properties of crystallizable polymeric material. Thus it is important to study the crytallinity properties of the composite after the addition of filler.

Liang et al. (2013) has studied the crystalline properties of PLLA composite filled with nanometer Calcium Carbonate. The results are shown in figure below

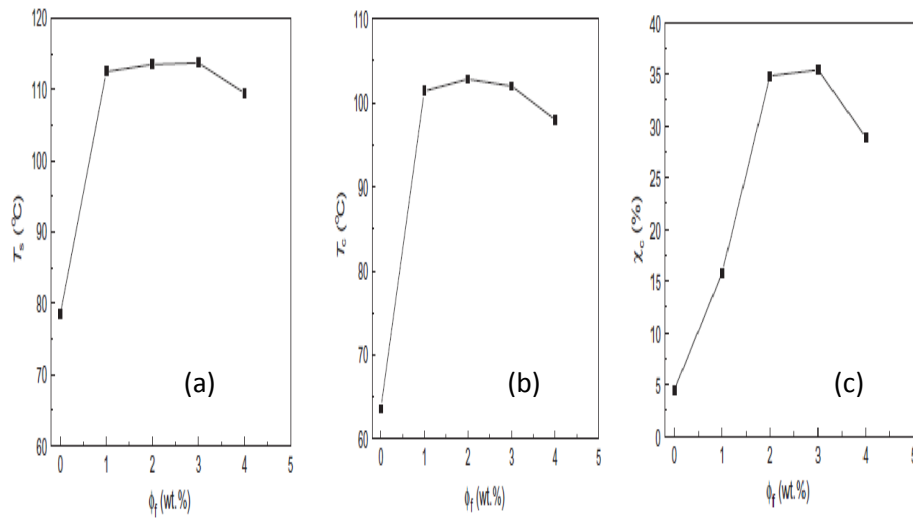


**Figure 2.5** a) Relation between onset temperature and nano  $\text{CaCO}_3$  weight fraction b) Relation between crystallization temperature and nano  $\text{CaCO}_3$  weight fraction c) Relation between degree of crystallinity and nano  $\text{CaCO}_3$  weight fraction

Crystallization onset temperature is the temperature that crystalline material starts to crystallize. In the figure above, it can be seen that the addition of  $\text{CaCO}_3$  give significant increase on the crystallization temperature compared to neat PLLA, with further addition of  $\text{CaCO}_3$  the onset temperature varies slightly but started to decrease when the filler content reach 4wt%.  $\text{CaCO}_3$  play the role of heterogeneous nucleation in PLLA matrix.

Crystallization temperature also follow the same trend as crystallization onset temperature as shown in Figure 2.5 (b).

In Figure 2.5 (c), it can be seen that the degree of crystallinity of composite increases with increasing filler content (wt%) when filler content is less than 3%. Further increase of the filler content, decrease the crystalline degree of the composite. This shows that at even though  $\text{CaCO}_3$  may play the role of nucleating agent. But this does not means that degree of crystallinity of the composite will be increasing with the increase of filler content as the crystalline degree also dependent on other factor. Liang *et al.* stated that the decrease of degree of crystallinity is due to the limited movement of PLLA molecular chain which also reduce the molecular chain for crystallization.

## CHAPTER 3

### METHODOLOGY

#### 3.1 Materials

*Lokan* Powders (Calcium Carbonate)

PLA

Chloroform

Extec liquid Releasing agent

#### 3.2 Instruments

Stainless steel mold ( 12 x 18 cm )

Magnetic Stirrer

Scanning electron microscope (SEM)

Field Emmision Scanning Electron Microscope

X-Ray Diffraction Spectrometer

Differential Scanning Calorimeter

Instron Universal Testing Machine

### **3.3 Methods**

#### **3.3.1 Preparation of *Lokan* Powder (LP) particle**

200 g of marsh clam shell (*Lokan*) were washed and scrubbed to remove the dirt from the shell. Then the shells were boiled in the boiling water for about 10 to 15 minutes. This may allows the shells and fleshes being separated easily. Again, the shells were scrubbed, cleaned thoroughly with distilled water and rinsed gently to remove the remaining pollutant that stick on the shells. Next, the shells were dried in the oven at temperature of 85°C for 24 hours. The cleaned and dried shells were then crushed by using manual mortar and pestle for the production of smaller aggregate. Small pieces of aggregates were then ground into powder form by using blender machine. The powders were then sieved through aperture size of 100  $\mu\text{m}$ , and were dried again for 1 hour at 75°C before packed and sealed in a polyethylene plastic bag.

#### **3.2.2 Preparation of PLA polymer solution**

PLA having a weight average molecucar weight ( $M_w$ ) of  $1.63 \times 10^5$  g/mol was obtained from Mitsui Chem Co. Ltd. Its polydispersity in weight- ( $M_w$ ) to number average ( $M_n$ ) molecular weight ratio ( $M_w/M_n$ ) was 1.82. PLA polymer solution were prepared by dissolving PLA powder into purrified chloroform at the ratio of 1:10. The solution were stirred using the magnetic stirrer for 12 hours to make the powder soluble completely. The solution were then left for 24 hours to ensure a sufficient dissolution and to get rid of the viscosity bubble.

### **3.2.3 Production of Thin Film Composites**

LP/PLA thin film composites were produced by hand-lay-up and open mold techniques. For control specimens, no LP filler was impregnated with PLA resin, (100% wt. percentage of PLA). Then, LP filler was blended with PLA resin by mixing them according to the composition of 2wt%, 4wt%, 6wt%, 8wt% and 10wt% LP in 100g solution. The mixing process is done by magnetic stirrer for sufficient time to produce homogenous solution. Then, the inner surface of the mold was treated with several layers of releasing agent. The mixture of PLA resin and LP filler was carefully poured into the mold, and cured.

### **3.2.4 Scanning electron microscopy (SEM)**

A Hitachi S3400N scanning electron microscope was used to investigate the surfaces of *Lokan* Shell and *Lokan* Powder Particle. The specimens were placed on an aluminium stub and sputter coated with a thin layer of Gold (Au) in order to avoid electrostatic charging during examination and observed under different magnifications. The SEM is connected with Horiba Emax EDX for elemental analysis of the sample.

### **3.2.5 Field Emission Scanning electron microscopy (SEM) study**

JEOL JSM-7600F field emission scanning electron microscope was used to investigate the open surface of LP/PLA composite. The material is placed in aluminium stub and observed with different magnifications.

### **3.2.6 Tensile testing**

Using the standard specimen of thin film, Dumbell shape with dimensions of ASTM D882 and tensile tests were also conducted according to ASTM D882. ASTM D882 shall be used whenever the width of specimen is less than 1mm. The specimen gage length of 250mm is considered as standard. The test was carried out using an Instron Universal Testing Machine Model 5569 at cross-head speed of 1 mm/min. Tensile properties were determined for five samples of each composition of LP .

### **3.2.7 X-ray diffraction analysis (XRD)**

X-ray diffraction (XRD) analysis was performed on a powder diffractometer. The XRD pattern were recorded in Pan Analytical Xpert instrument using Cu ( $K\alpha$ ) radiation with wavelength  $1.54 \text{ \AA}$  at room temperature in the range of  $2\theta$  and equipped with diffracted software. X-ray diffraction provides the information by evaluated the presence of the layered structure of the nanoclays and calculated the distance between the layers. This analytical tool probes the crystal lattice structure of the nanocomposite. An x-ray is projected into the sample. The distance between the waves as they exit the sample is due to the diffraction of the waves by the basal plane. This d-spacing refers to the spacing between planes of the crystal lattice. When different lattice structure or spacing between the platelets is present, there will be multiple peaks on the resulting graph.

### **3.2.8 Differential Scanning Calorimeter (DSC) Analysis**

In order to investigate the effect of LP loading on degree of crystallinity of the matrix, Differential Scanning Calorimeter (DSC) analysis were performed. Differential Scanning Calorimeter (DSC) analysis is done using model Mettler Toledo DSC 821 e. The crystallization behaviour of the composite is studied at the temperature range of 30-300°C under nitrogen atmosphere with a heating rate of 10 °C/min.

## CHAPTER 4

### RESULTS AND DISCUSSION

#### 4.1 Characterization of *Lokan* Shell Powder

##### 4.1.1 Identification of type of polymorph by XRD analysis

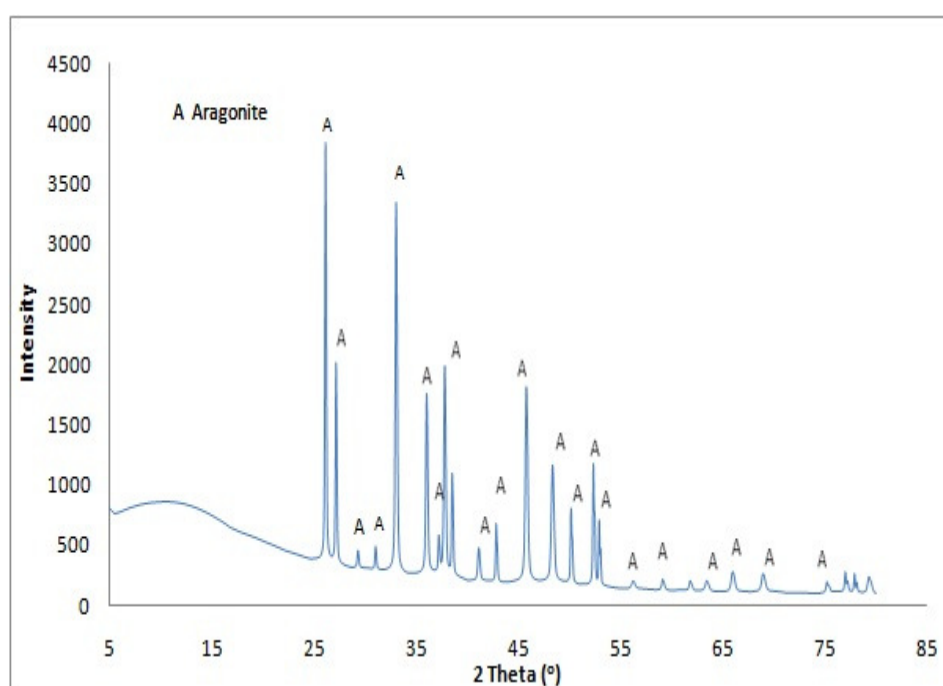
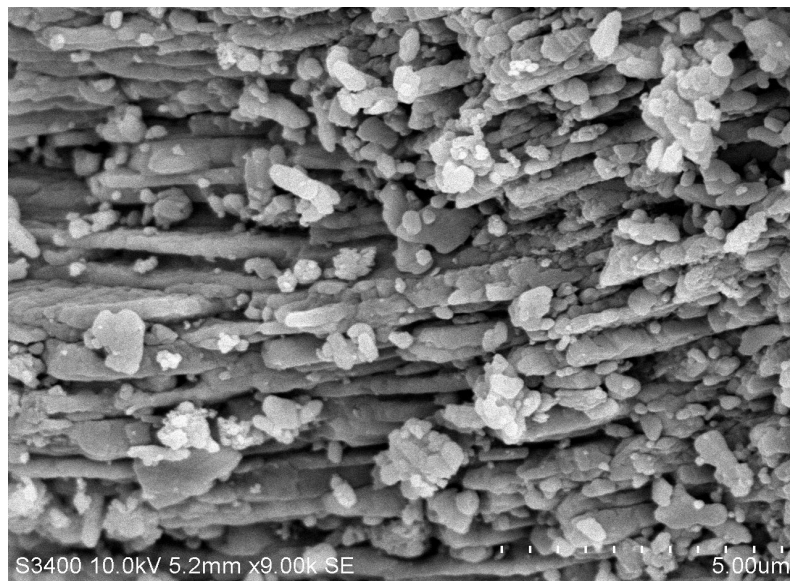


**Figure 4.1** XRD patterns of the *Lokan* shell powder.

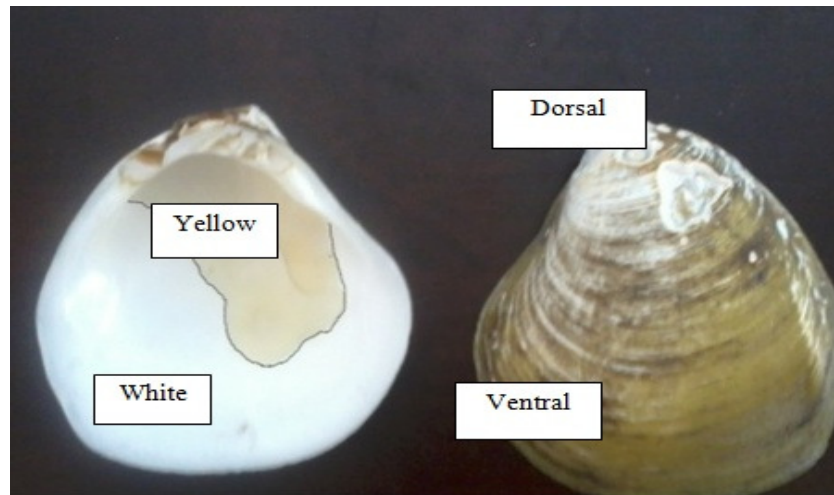
Figure 4.1 illustrates XRD patterns of the calcium carbonate from the *Lokan* shell powder. All the peak matched the aragonite peaks (Reference code 00-041-1475) indicating that *Lokan* shell contain entirely aragonite.

#### 4.1.2 Surface morphology by SEM

Figure 4.2 reveals the surface morphology of *Lokan* shell powder studied by SEM. Micron-sized of calcite and aragonite forms were detected in the powder. The rod-like aragonite crystal powders were noticed to be attracted among each other, producing cluster of many particles and the particles are arranged properly in similar orientation. This may due to high surface energy, which results in high attraction among the particles. The particle-particle interaction phenomenon was also addressed by many authors (He *et al.*, 2011; Zhang *et al.*, 2008) which was normally occur among untreated (uncoated) calcium carbonate powder due to Van der Waal force of small particles.



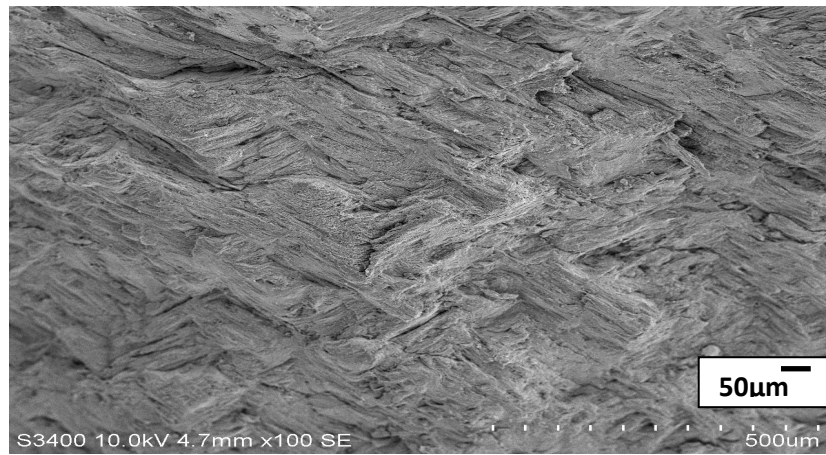
**Figure 4.2** The surface morphology of the *Lokan* shell powder



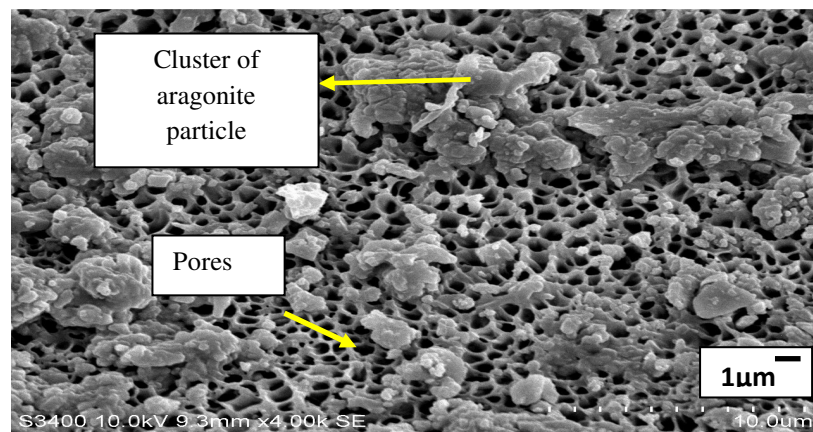
**Figure 4.3** The surface morphology of the inner and outmost surface

Figure 4.3 shows the image of the outmost and inner surfaces of the *Lokan* shell. The outer surface or periostracum layer of the shell is rough and the presence of concentric ring is detected. At the ventral part of the shell, the eroded umbo surface is present and darker green colour is seen. At the inner surface or nacreous layer, yellow colour area was detected at the dorsal part where the muscles attached whereas other part is in white colour.

Figure 4.4-4.8 shows the morphology of three different parts of the *Lokan* shell. The cross-sectional part of the shell (Figure 4.4) reveals that the aragonite layers were arranged in the form of cross-lamellar structure. Porous surface was detected at the ventral part (Figure 4.5) of the outmost layer of the shell whereas finer structure was at the dorsal part (Figure 4.6). Different aragonite size was found at the inner part of the shell. Coarser aragonite polymorph (Figure 4.7) was identified at the yellow colour area at the dorsal part of inner surface compared to white area surface (Figure 4.8) of the shell.



**Figure 4.4** Cross-sectional area



**Figure 4.5** Ventral part of the outmost surface

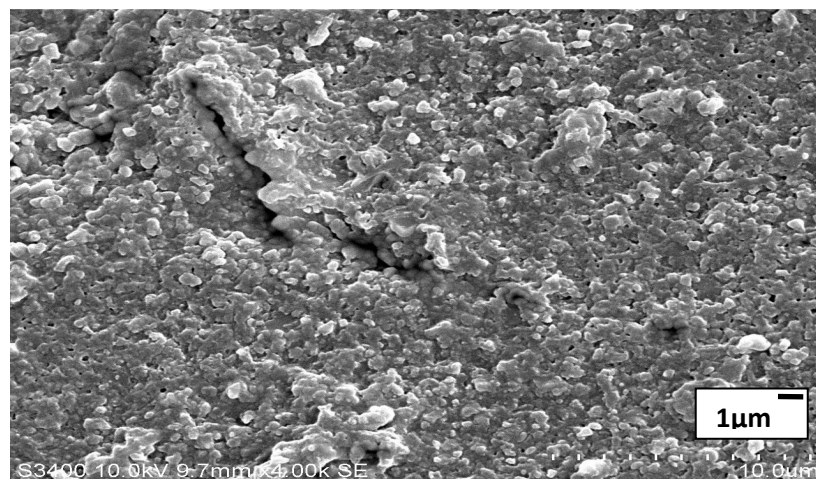


**Figure 4.6** Dorsal part at the outmost surface



**Figure 4.7** Yellow colour area of the dorsal part at the inner surface

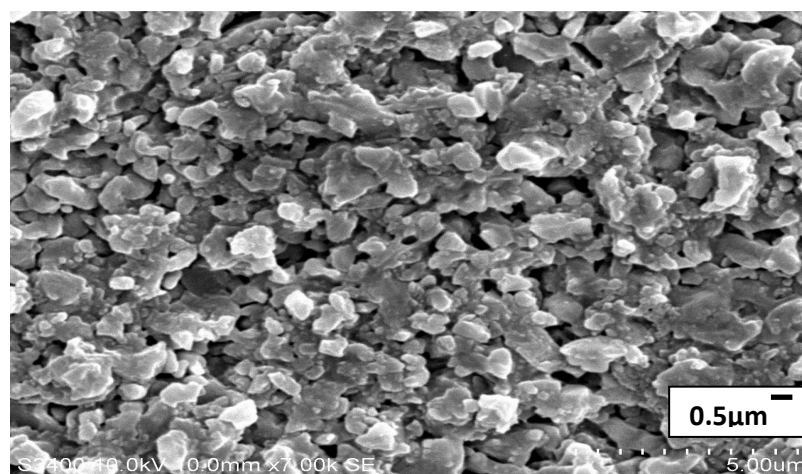


**Figure 4.8** White colour area of the dorsal part at the inner surface of the *Lokan* shell.

#### 4.1.3 Elemental analysis by EDX

Table 4.1 shows the EDX result of elemental content of the powder derived from *Lokan* shells. The findings showed that the powder which is less than 63  $\mu\text{m}$  contain pure calcium carbonate without any trace element. Calcium carbonate of the powder was rich of oxygen and calcium.

**Table 4.1** Elemental content of powder derived from *Lokan* shell

Spectrum	C (%)	O (%)	Ca (%)	Total
Spectrum 1	11.23	33.69	55.08	100
Spectrum 2	15.94	50.63	33.43	100
Spectrum 3	15.38	45.37	39.25	100
Mean	14.18	43.23	42.59	
Std. Deviation	2.58	8.67	11.20	
Max	15.94	50.63	55.08	
Min	11.23	33.69	33.42	

Comparing with result obtained by Nurul Islam *et al.* (2011), like cockle shell, *Lokan* shell also contain of higher amount of carbon and calcium compared to commercial Calcium Carbonate. As both shells contain aragonite and commercial Calcium Carbonate contain calcite it can be concluded that the amount of carbon and calcium in aragonite is higher than the amount of carbon and calcium in calcite. In aragonite, both Ca and O are high due to formation of aragonite as a result of pre adsorption of organic substrate. This requires strong Ca and O interaction with the substrate surface. The acid or alkali treatment of these surfaces increased the amount polar functional group which has strong interaction with polar organic molecule through hydrogen bond. This resulted in the accumulation of organic molecule on surface, hence induce the nucleation of aragonite crystal ( Nurul Islam *et al.* ,2011).

#### 4.1.4 Comparison of polymorph from different species of bivalves

Table 4.2 shows the comparison of the polymorph of other mollusc shells studied by other researchers with *Polymesoda expansa*.

Nurul Islam *et al.* (2011) found that there were other trace elements found in *Anadara granosa* shell powder such as Al, Cu and Te after the powders were sieved with aperture size of 90 µm. Compared to *Anadara granosa*, *Polymesoda expansa* does not contain any trace element for the powder passed through 63 µm sieve size. *Strombus gigas* shell from a family of *Strombidae* was dominantly contain aragonite. Calcite was only found at the outmost layer of the *Strombus gigas* shell.

**Table 4.2** Polymorph of different species of bivalves shell.

Polymorph	Family	Species
Entirely Aragonite	Unionidae <sup>a</sup>	<i>Amblema costata</i> , <i>Elliptio dilitatus</i> , <i>Fusconia subrotunda</i> , <i>Fusconia undata</i> , <i>Legumia recta latissima</i> , <i>Megalonaias gigantean</i> , <i>Pleurobema cordatum</i> , <i>Plelhobasus cyphyus</i> , <i>Quadrula pustulosa</i> , <i>Quadrula quadrula</i> (Compere,1973)
	Lampsilinae <sup>a</sup>	<i>Actionaias carinate</i> , <i>Lampsilis anadontoides</i> , <i>Lampsilis ventricosa</i> , <i>Leptodea fragilis</i> , <i>Obovaria subrotunda</i> , <i>Obliquaria reflexa</i> , <i>Proptera alata</i> , <i>Ptychobranhus fasciolaris</i> , <i>Trucilla donaciformis</i> (Compere,1973)
	Anodontinae <sup>a</sup>	<i>Lasmigona complanata</i> , <i>Lasmigona costata</i> , <i>Strophitus rugosus</i> (Compere,1973)
	Arcidae	<i>Anadara granosa</i> (Nurul Islam et.al,2011)
	Corbiculidae <sup>b</sup>	<i>Polymesoda bengalensis</i>
Calcite and Aragonite	Strombidae <sup>c</sup>	<i>Strombus gigas</i> Linnaeus (Compere,1973)
Entirely calcite	Ostreidae <sup>c</sup>	<i>Ostrea sp</i> (Compere,1973)

<sup>a</sup>The samples were taken from the Muskingum River in Ohio.

<sup>b</sup>The samples were taken from Kota Samarahan, Sarawak, Malaysia.

<sup>c</sup>The samples were taken from the Muskingum River in Nujol.

## 4.2 Characterization of PLA/LP composite

### 4.2.1 X-Ray Diffraction Analysis

XRD pattern are shown in Figure 4.9-4.12.

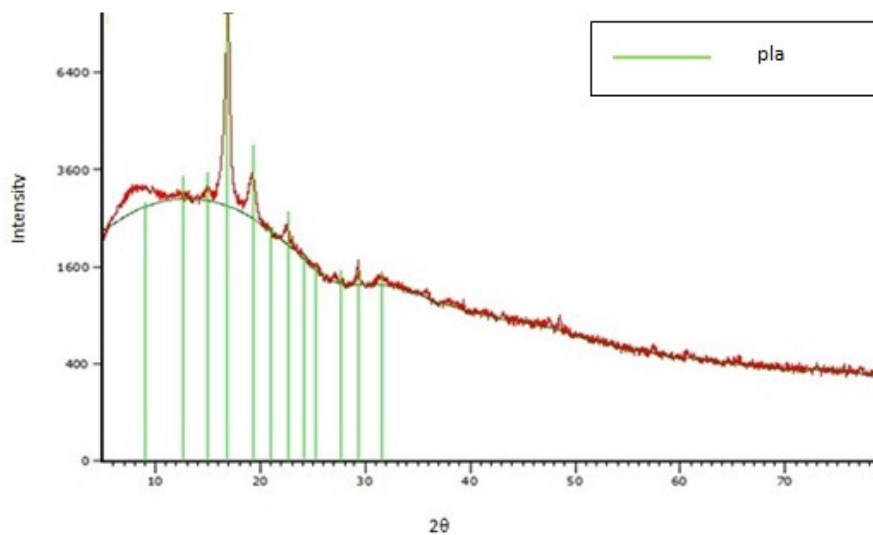


**Figure 4.9** XRD pattern of neat PLA

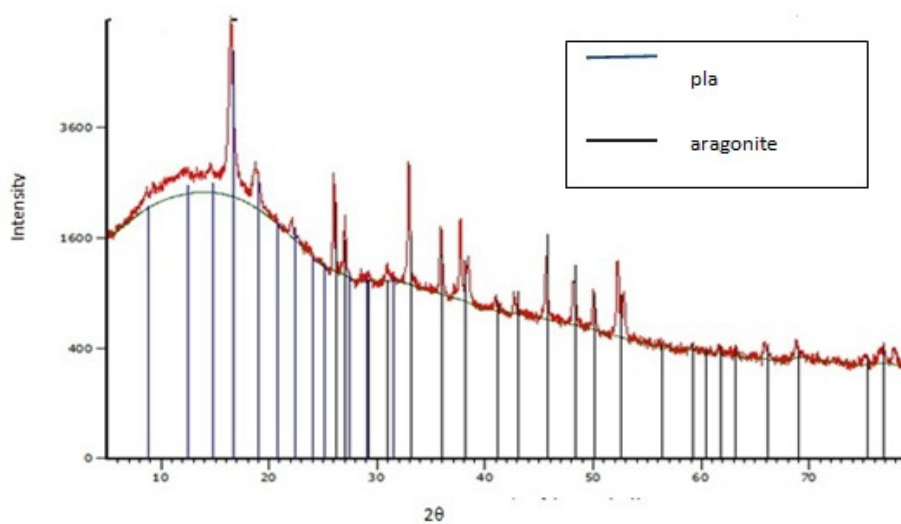


**Figure 4.10** XRD pattern of PLA/LP composite with 2wt% filler content

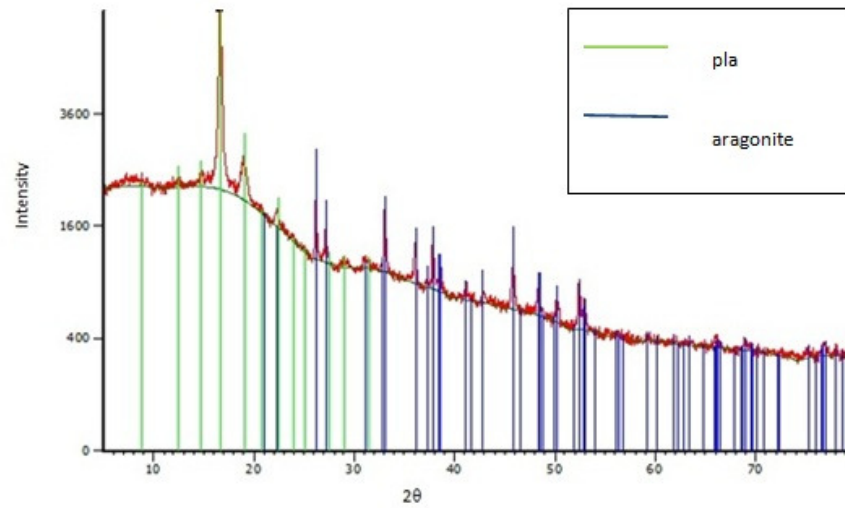


**Figure 4.11** XRD pattern of PLA/LP composite with 6 wt% filler content

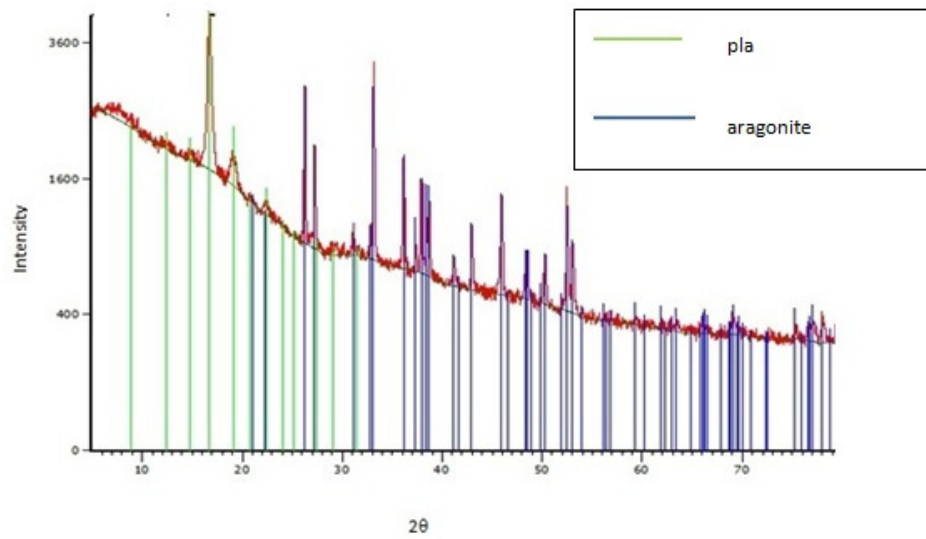


**Figure 4.12** XRD pattern of PLA/LP composite with 10 wt% filler content

Figure 4.9 shows the XRD pattern of pure PLA. The pattern matched the peak of Poly D-Lactide ( Reference code 00-041-1917) .The peak of PLA is shown at the range of 12-32° and have the highest intensity of 5810.77.

With the addition of LP filler, the Aragonite Calcium Carbonate (Reference code 00-041-1475) peak is started to shown. In Figure 4.10, at 2wt% filler content, the peak of PLA is shown at the range of 12°-30 °, with the highest intensity of 4086.74 while the peak for aragonite is shown at the range of 22°-78°, with the highest intensity of 1895.56.

In Figure 4.11, with the addition of 6wt% filler, the same trend of pattern as in figure 4.10 is observed. In this figure, the peak of PLA is shown at the range of 16°-30°, with the highest intensity of 4086.74 while the peak for aragonite is shown at the range of 22°-79°, with the highest intensity of 1987.2447.

Meanwhile, Figure 4.12 shows the XRD pattern with the highest filler content which is 10wt%. In this pattern, PLA peak start to shown at 14°-28° and aragonite at 19°-78°. The highest intensity of PLA is 2340.26 for aragonite the highest intensity is 2444.67. It can be seen that intensity of PLA in this sample has drop more that 50% of the intensity of neat PLA.

From all patterns, it can be seen that the addition of LP filler will decrease the intensity of PLA and increase the intensity of Calcium Carbonate crystal. Intensity is also dependent on the degree of crystallinity. The crystallization behaviour of the composite is further discussed below.

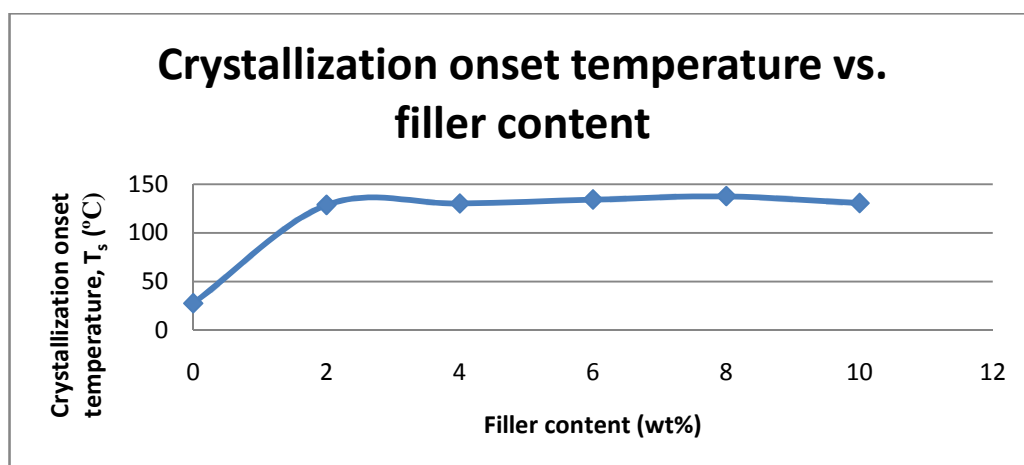
#### **4.2.2 Crystallization behaviour**

The crystalline properties of PLA/LP composite were measured using a differential scanning calorimeter, to identify the influence of the particle content on the crystalline properties.

**Table 4.3** Summary of result from DSC analysis for all sample.

Sample (wt%)	Crystallization onset temperature, $T_s$ (°C)	Crystallization temperature, $T_c$ (°C)	Degree of crystallinity, $\chi_c$ (%)	Enthalpy of fusion (J/g)
0	27.70	142.49	27.70	24.93
2	128.67	142.91	22.41	20.169
4	130.13	143.76	24.16	21.744
6	134.18	143.60	23.88	21.492
8	137.59	146.30	12.17	10.953
10	130.54	143.52	15.72	14.148

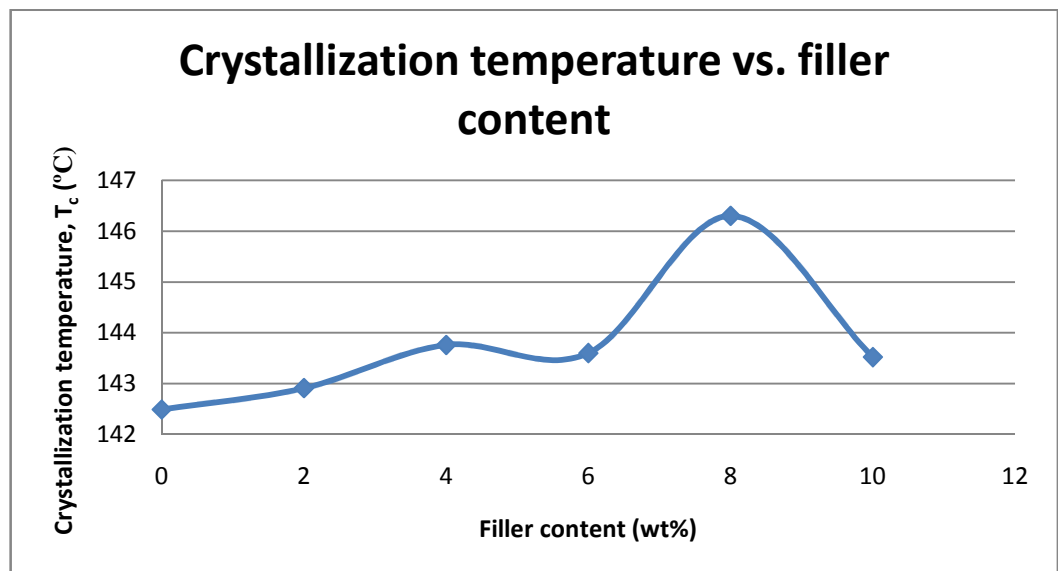
Crystallization onset temperature is the temperature that recrystallization starts on crystalline materials. The onset temperature is an important parameter to demonstrate crystallization properties on polymeric material.



**Figure 4.13** Crystallization onset temperature vs. filler content

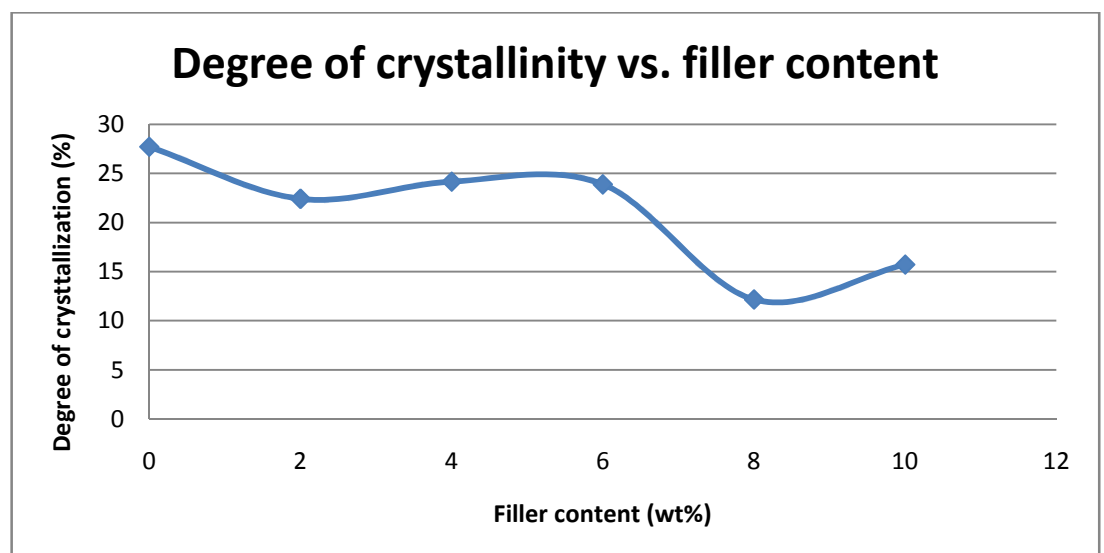
Figure 4.13 shows the relation between crystallization onset temperatures,  $T_s$  with filler content. From the result, it is observed that the value of  $T_s$  of the filled PLA composite system with 2wt% filler is obviously higher than that of the neat PLA, and then it varies slightly with an increase of filler content. This indicates that the addition of LP filler increase the crystallization onset temperature of the filled PLA composite.

From the result, it can be said that the calcium carbonate particle may play the role of nucleation agent in the PLA matrix (Liang *et al.*, 2013). Liang *et al.* research in 2013 lead to same result as current research and they also state that as the calcium carbonate play the role of heterogenous nucleation in PLLA matrix, it is beneficial to start the recrystallization of composite at higher temperature. This lead to the increase of crystallization onset temperature when the filler of PLLA composite increase.



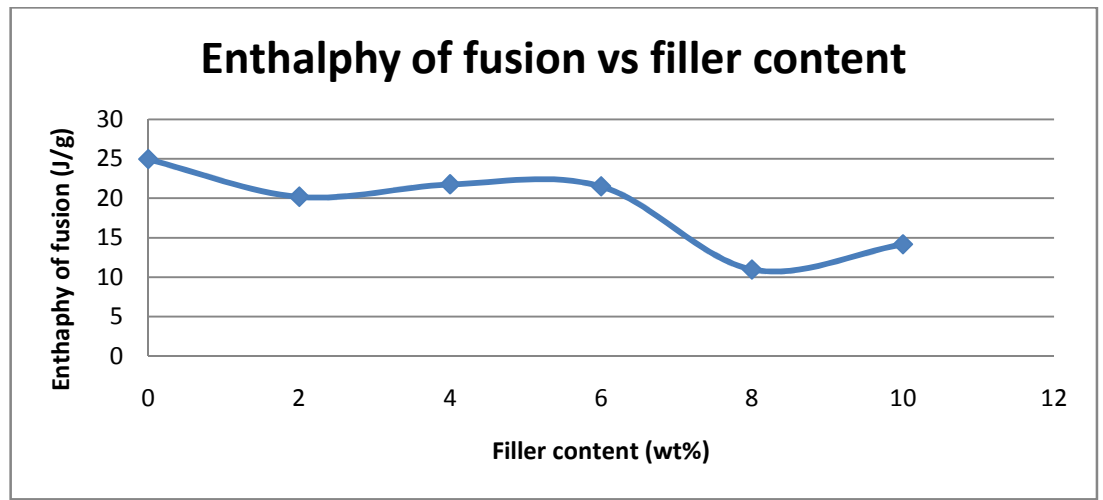
**Figure 4.14** Crystallization temperature vs. filler content

Figure 4.14, indicates the crystallization temperature relation with filler content. From here we can see that, the temperature increase from 0-4 wt% filler content, slightly decrease at 4-6wt% and reach maximum crystallization temperature at 8wt% filler content, before started to decrease with the further increase of filler content. However the difference between the crystallization temperatures of all samples is small. This shows that filler content, does not give a significant impact on the crystallization temperature of the composite. Liang *et al.* (2013) has observed different pattern in his research where the addition of filler in the composite increase the crystallization temperature significantly when 1wt% filler content is added to the PLLA matrix, and it slightly varies with the addition of filler content. The increase of crystallization temperature in his research is related to the increase of onset crystallization temperature with the addition of filler content while in current research, the crystallization temperature is not dependent on the crystallization temperature as both result shows different pattern.



**Figure 4.15** Degree of crystallinity vs filler content (wt%)

Figure 4.15 show the relationship between degree of crystallinity with filler content (wt%) . As seen in Figure 4.15 , the addition of filler brings negative effect to the degree of crystallinity of the composite. At the addition of 2wt% filler, the degree of crystallinity drop, and the value varies slightly from 2-6wt% .However at 8wt% filler content, there is a sharp drop in the degree of crystallinity it gives give the lowest value of degree of crystallinity among all samples.



**Figure 4.16** Enthalpy of fusion (J/g) vs filler content (wt%)

It is known that heat of fusion of semi crystalline polymer can be related to their degree of crystallinity from the equation;

$$\chi_c = (\Delta H_c / \Delta H) \times 100\% \text{ (Nampothiri et.al, 2010)}$$

Where  $\Delta H_c$  is the thermal enthalpy during crystallization of the composite and  $\Delta H$  is the thermal enthalpy of crysallization for crystalline PLLA homopolymer = 93.16 J/g. As  $\Delta H$  is a constant value, the crystallization heat of fusion for the composite is dependent on the degree of crystallinity value. As shown in Figure

4.16, the pattern of the graph follow the pattern of the graph in Figure 4.15, where there is a drop in crystallization heat of fusion for the composite with the addition of filler and show the lowest enthalphy at 8wt% filler content.

The result however, is slightly difference from the result of Liang *et al.* ( 2013) . In his research, the degree of crystallinity increase for the filler content under 3wt% and started to decrease slightly with the addition of more filler. His finding indicates that the role of nucleating agent in of nano-  $\text{CaCO}_3$  particle under 3wt% filler content is obvious.

Meanwhile, in current research, although LP filler also plays the role of nucleating agent in the PLA matrix, but the limited movement of the PLA molecular chain and the decrease number of molecular chain play more role to the degree of crystallinity of the composite. Hence resulted in the decrease of degree of crystallinity of the sample with the addition of filler content. As discussed in the XRD analysis of composite, the intensity of PLA and  $\text{CaCO}_3$  crystal is also dependent on degree of crystallinity of PLA matrix. It can be seen from the result that, the degree of crystallinity of PLA matrix decreased with the increased of filler content. This decreased in degree of crystallinity, also decreased the intensity of PLA, hence increased the intensity of  $\text{CaCO}_3$ .

#### **4.2.2 Tensile Properties**

The results obtained from tensile testing are shown in Table 4.4. Elongation at break (%), Young Modulus, Tensile Strength, and Tensile Energy Absorption of PLA with different composition of LP filler can be analyzed from the tensile test

results. The table includes results of all specimens with different filler content and also of neat PLA resin sample for comparison purpose.

**Table 4.4** Summary of Tensile Result

Sample (wt%)	Elongation at break (%)	Young's Modulus (MPa)	Tensile strength (MPa)	Tensile energy absorption ( N/mm)
0	102.097	254.001	11.72	4.536
2	68.104	303.317	11.163	2.946
4	34.163	502.257	10.634	1.28
6	21.732	695.523	10.635	0.869
8	7.299	734.212	9.796	0.247
10	5.704	856.021	10.435	0.164

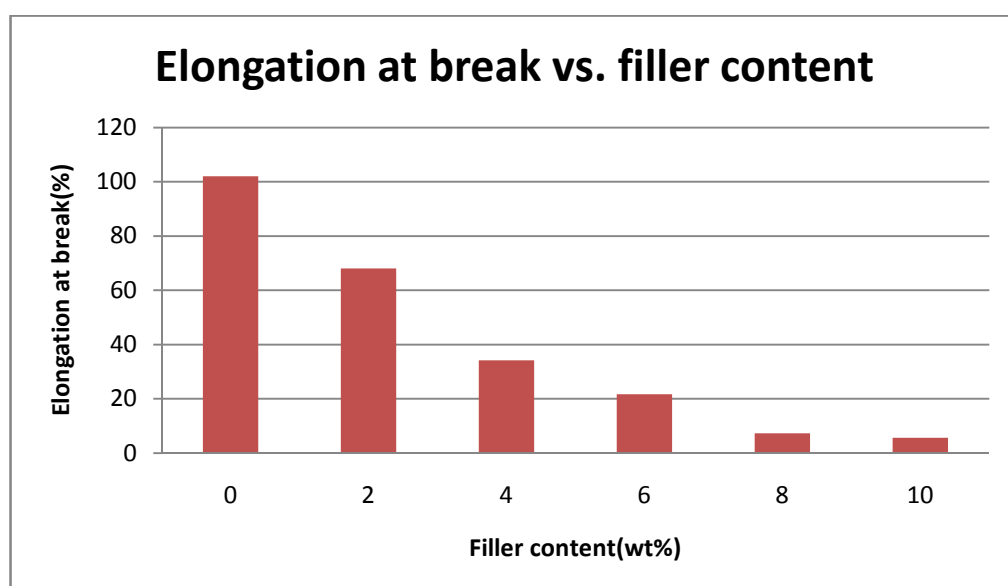


**Figure 4.17** Relationship between elongation at break and filler content

From Figure 4.17, it can be seen that the elongation at break for PLA/LP composites decrease substantially until 8wt% filler content when compared to neat PLA without filler. For 10% filler content, there is also a decrease in the elongation at break of the composite but the change of value is smaller compared to the change in the % of elongation at break from 0wt% to 8wt% filler content. The addition of LP decreases the ductility of the sample. For neat PLA, the specimen yielded with the most noted stress whitening band (craze) perpendicular to the tensile direction of the filler and fractured with small amount of necking. For neat PLA, ductile fracture is observed while for PLA/LP composite, brittle fracture are observed. The fracture of (a) neat PLA and (b) PLA/10wt% LP is as shown in Figure 4.18.

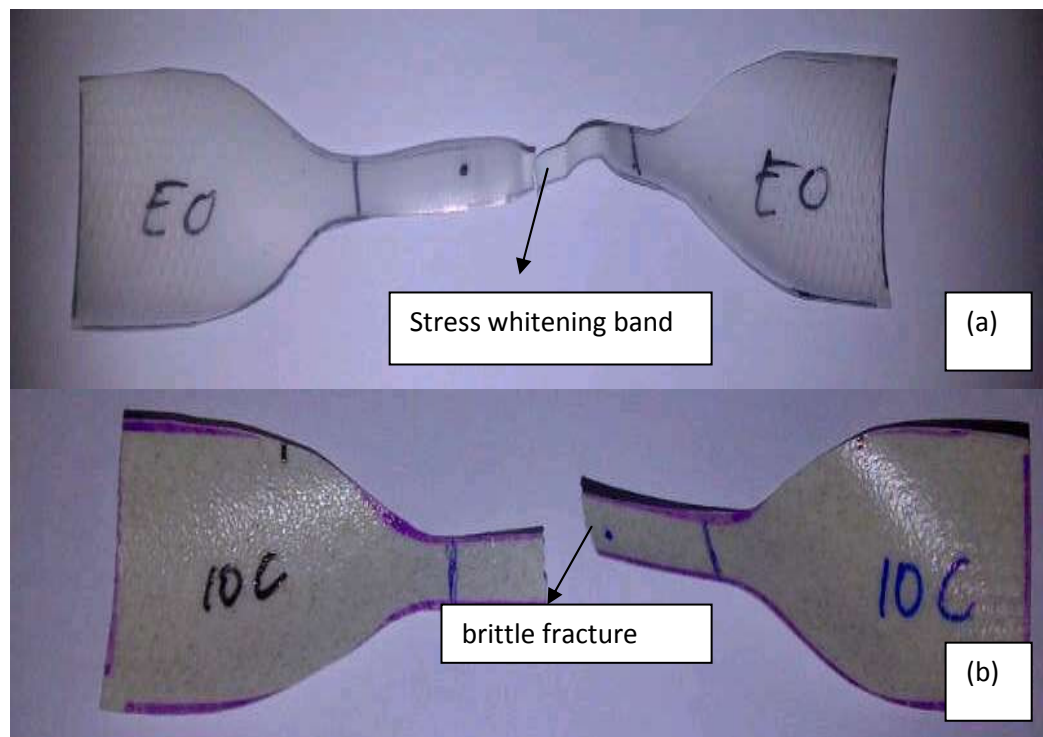


**Figure 4.18** (a) neat PLA sample after fracture (b) PLA/LP sample after fracture

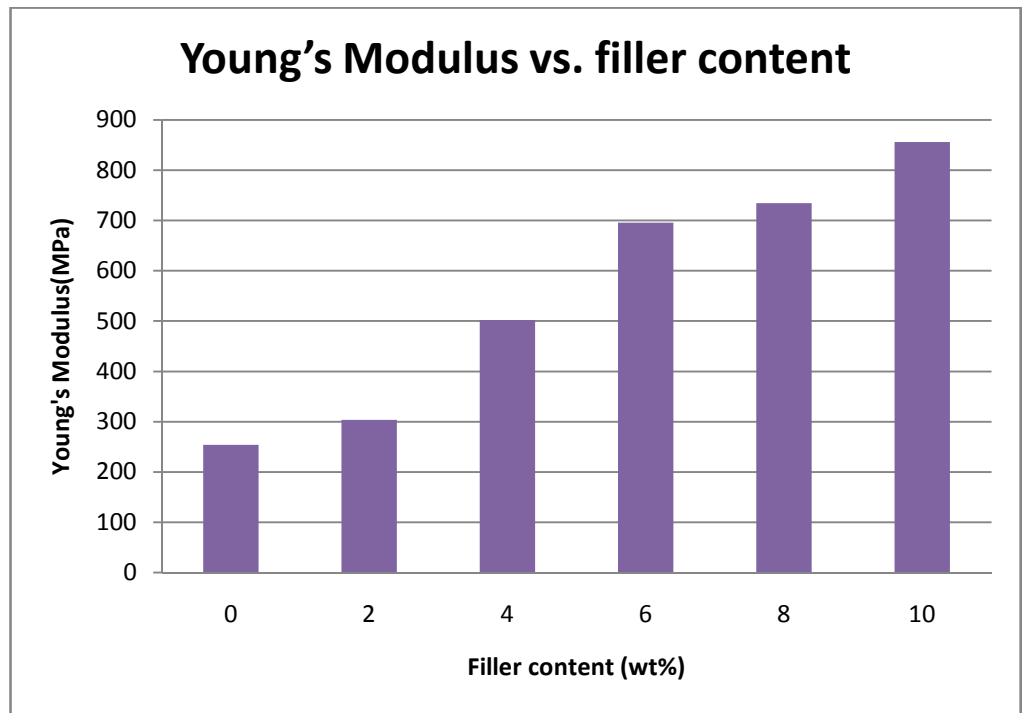


**Figure 4.18** Relationship between Young's Modulus and filler content

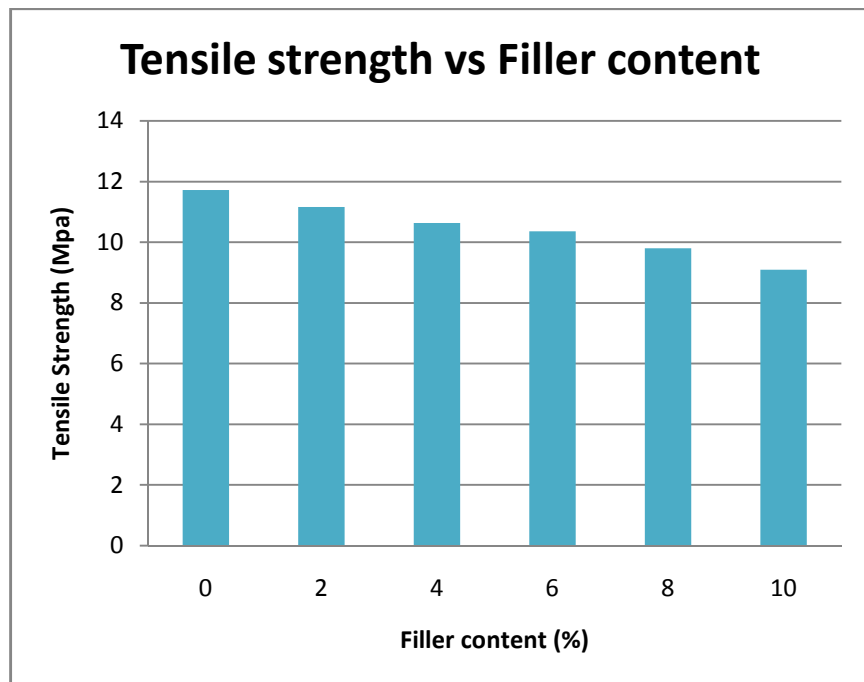


**Figure 4.19** Relationship between tensile strength and filler content

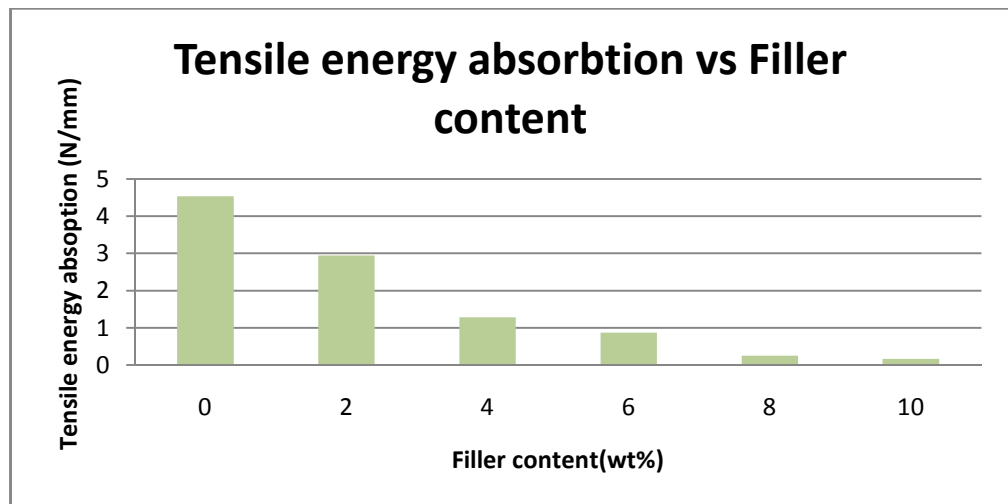


**Figure 4.20** Relationship between tensile energy absorption and filler content

Figure 4.19 show the result of Young's Modulus vs filler content. Young's Modulus is a measure of stiffness of an elastic material. It predicts how much material can extend under tension. From the graph, it can be seen that Young's Modulus of the composite increase with the increase of filler content. Addition of LP filler in PLA composite resulted in stiffer material. Young's Modulus is also related to degree of crystallinity of the material. In general, the higher the Young's Modulus, the higher the degree of crystallinity. However, in this research, the value of Young's Modulus is found to increase with the decrease of degree of crystallinity. This indicate that, the use of *Lokan* Powder as filler may resulted in the formation of small and imperfect crystal during crystallization. This small and imperfect crystal lower the degree of crystallinity of PLA matrix and also decreased Young's Modulus resulted in stiffer but brittle composite material.

Meanwhile, in Figure 4.20, the tensile strength of the composite decrease with increasing of filler content. However the decrease is unsubstantial, where the

difference between the tensile strength of the composite is only  $\pm 2$ MPa. The tensile strength of the composite is almost independent of the filler content.

Figure 4.21 shown the relation between tensile energy absorption of the composite with filler content. From the graph it can be seen that the energy absorption of the composite decrease with the increment of filler content compared to neat PLA polymer. This is true, due to the fact that LP filler contain  $\text{CaCO}_3$  which is a brittle ceramic. Addition of LP filler induce brittle properties to the composite, when a composite lose its ductility it also lose the capability of absorbing much energy before failure.

The result is supported by the result in other journal which indicate that the percentage of elongation at break for PLLA/nanosized calcium carbonate composite were also decrease with the increase of filler percentage. ( Jiang et al. ,2007). Jiang et al. also stated that all the neat PLLA specimen fractured without necking and all the PLLA/NPCC yielded with noticeable stress whitening across the gage length. Where in current research, stress whitening is most noticeable in neat PLA and at the maximum amount of filler content, 10wt% the stress whitening is almost unnoticeable. The massive craze in his result was resulted by the debonding at the particle surface which decrease the plastic resistance of matrix below the applied stress due to release of strain constrain.

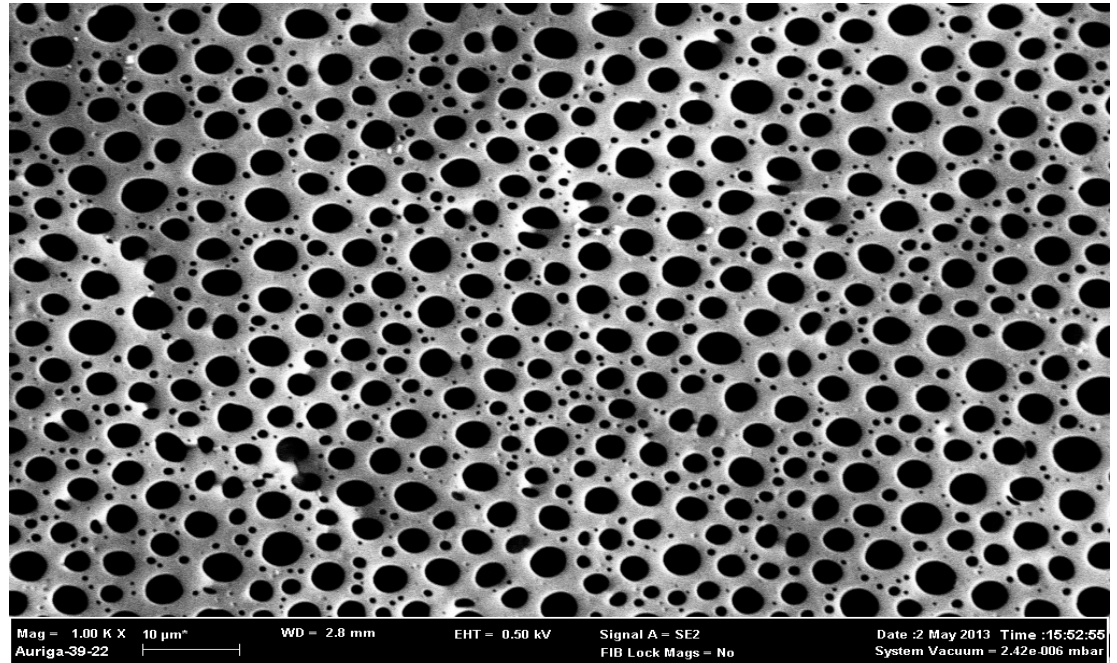
Debonding may also resulted in the decrease of tensile strength of material, in Jiang et al. research; he stated that in the system where interfacial adhesion is not high, debonding may occur at lower tensile stress than Yield strength of neat polymer which lead to substantial decrease of the tensile strength when filler

loading is increased. In current research, although there are decrease in tensile strength with the increase of filler loading, the decrease is only  $\pm 2$  Mpa for all specimen. Thus, the debonding issue in all samples is not prominent. Compared to Jiang et al. research, the debonding of his composite are due coating of stearic acid on the particle which limit the interaction between the filler and matrix. In current research, no coatings of stearic acid were done to all the samples.

In his result, Jiang et al. also found that the Young Modulus, increased with the increase of filler loading. This is equivalent with the result from current research. However, in Jiang et al. research the Young Modulus has only slight increase where in current research the increase is significant. As Young Modulus is the measure of how material can extend under tension, the result is also resulted by the bonding of matrix and filler in the sample. Jiang research has only slight increase due to debonding in his composite, where the interaction between the filler and matrix is weaker compared to in the current research. Current research, shows the good interaction between matrix and filler, and well dispersion of LP filler in PLA matrix, thus the composite with higher filler content can only have a slight change of shape after load is released.

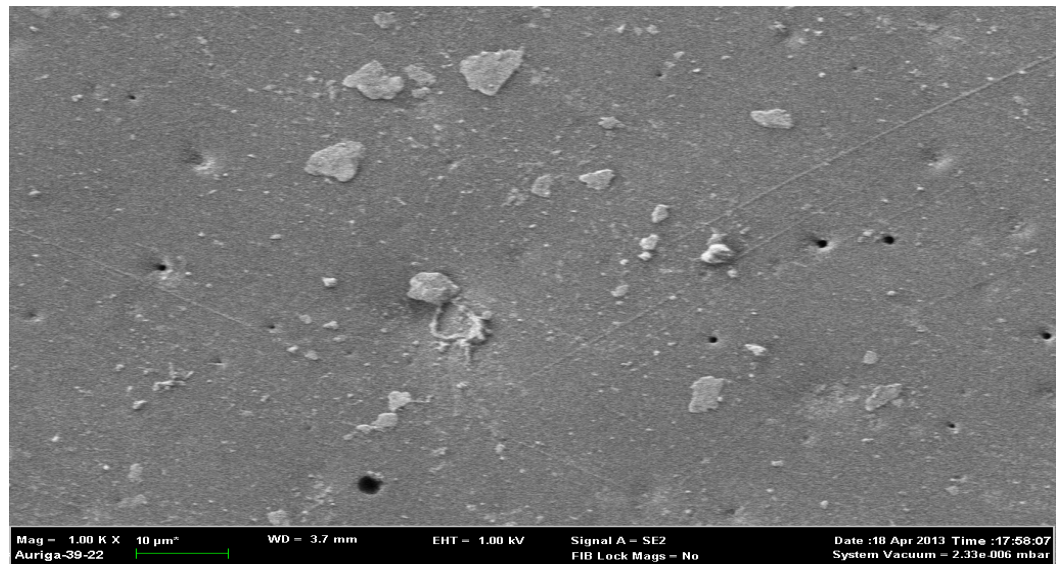
#### 4.2.2 Surface morphologies of PLA/LP composite

FESEM machine was used to study the surface morphology of the PLA/LP composite at different filler content.



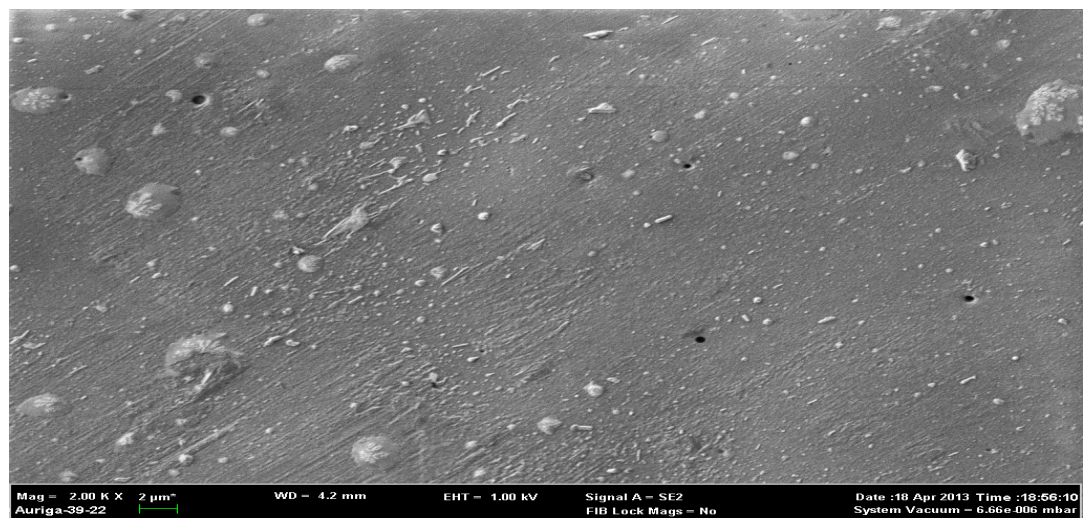
**Figure 4.22** FESEM of neat PLA

The surface morphology of pure PLA shows that neat PLA is highly porous structure. Even with low magnification, the porosity of neat PLA is clearly shown. The porosity of PLA, other than its biodegradable properties made it the choice of polymer to be used in biomedical and for implant. However, in certain application suitable level of porosity is needed, thus the implementation of LP filler to PLA matrix may change the porosity level of the PLA to suits the need of application.



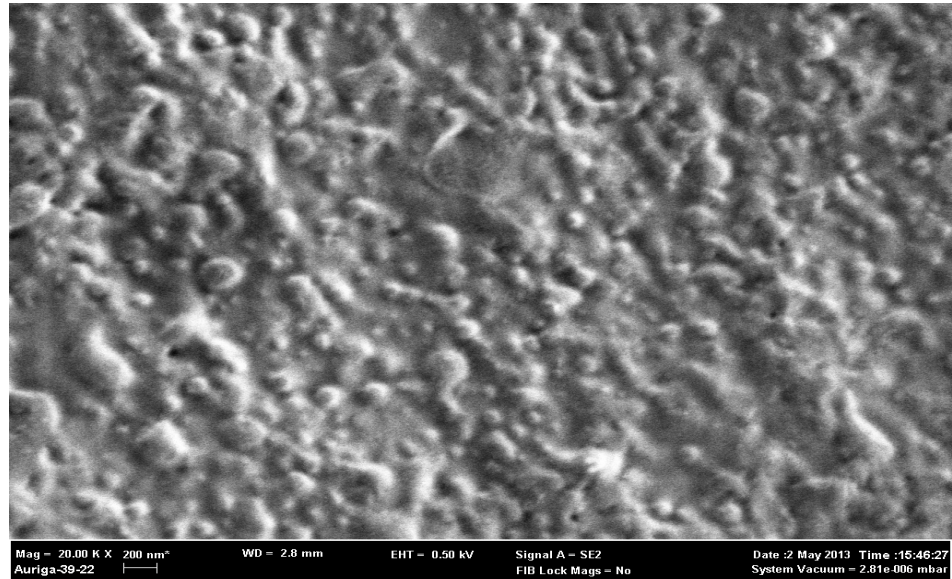
**Figure 4.23** FESEM of PLA/2wt% LP

As shown in Figure 4.22, with the addition of 2% LP filler, there is a decrease in porosity. The filler particle in PLA matrix is started to shown in at the surface. The filler is not well distributed in the matrix and particle agglomerate between each other. However, no debonding were detected, showing that there is strong connection between filler and matrix



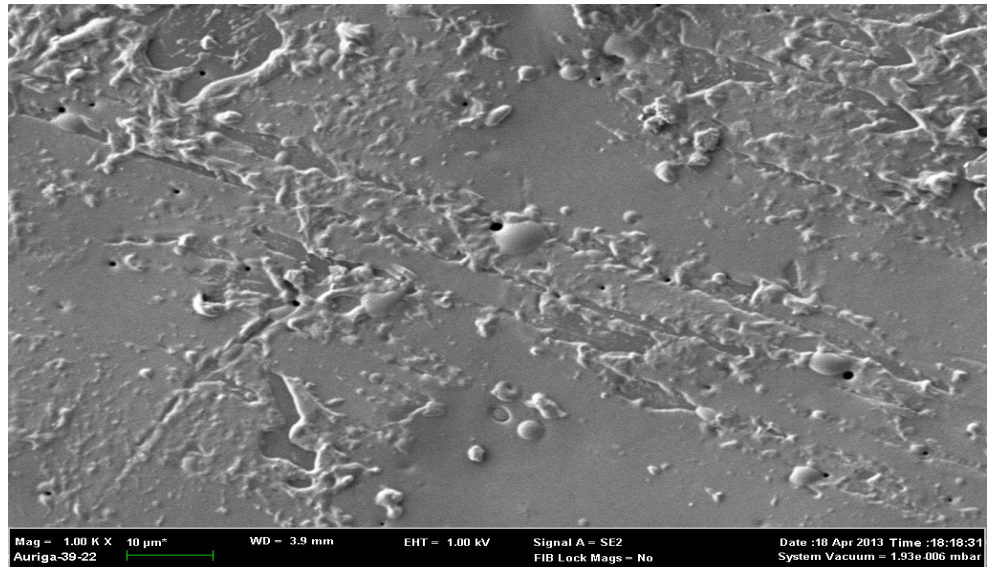
**Figure 4.24** FESEM of PLA/4wt% LP

In Figure 4.24, more particle can be seen as there are higher amount of filler in this composite. The filler is also not well distributed in the matrix but no debonding were detected. The agglomeration of particle also exist in the sample.



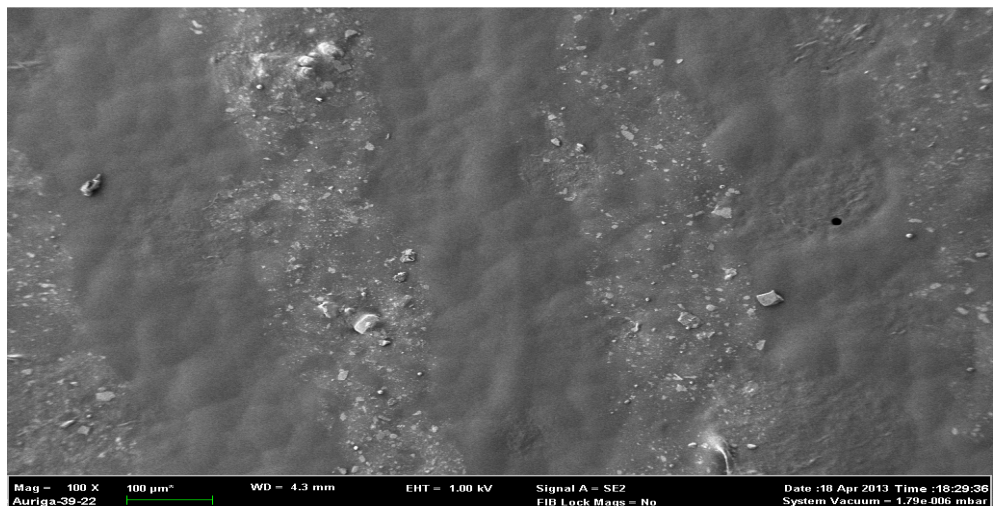
**Figure 4.25** FESEM of PLA/6wt% LP

Figure 4.25 shows the surface morphology of 6wt% LP filler. Better distribution of LP particle is seen in this composite surface compared to others. In this composite also, no debonding were detected and particle agglomeration also exist.



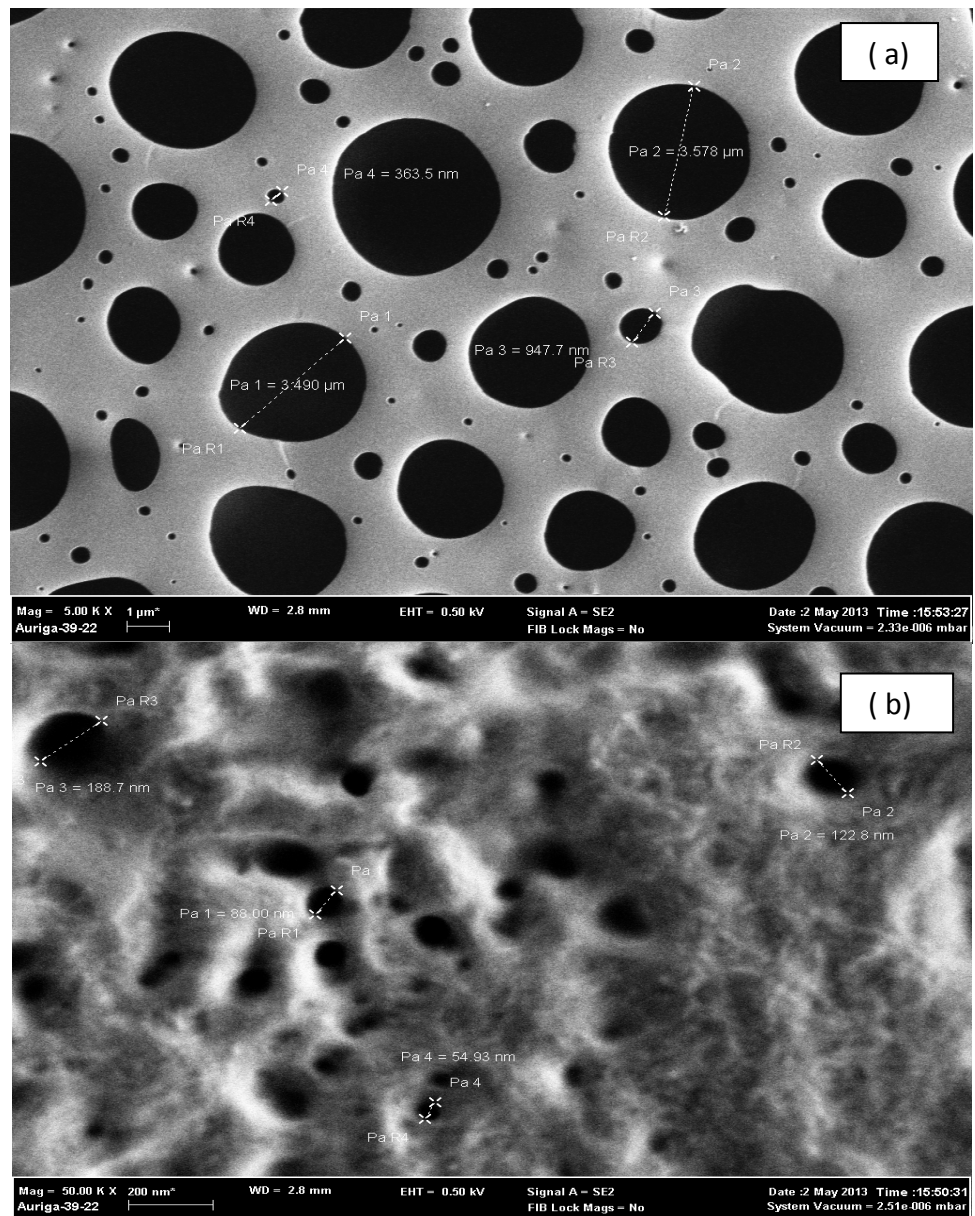
**Figure 4.26** FESEM of PLA/8wt% LP

Figure 4.26, also shows the same result as other figures, where no debonding were found and agglomeration of particle exist. There is also poor distribution of the particle.



**Figure 4.27** FESEM of PLA/10wt% LP

Meanwhile Figure 4.27 showed highest number of particles due to the high content of filler in this composite, 10wt%. The particle is still non-uniformly distributed.



**Figure 4.28** (a) FESEM at higher magnification of neat PLA (b) FESEM at higher magnification of PLA/6wt% composite.

Figure 4.28 (a) shows the FESEM morphology of neat PLA. The pore size is from 365nm -3.5 $\mu$ m. When 6% filler content is added, the pore size also decreased with to 54.3nm-188.7nm. The amount of pores have also decrease significantly when LP filler is added. The decrease of amount of pores also lead to the increase of Young Modulus of Material. Low porosity will leads to stiffer material. This support the result from tensile stress where Young Modulus increase with the increase of filler content.

The porosity increment with the increment of LP filler follow the same trend with the research done by Liu *et al.* Liu *et al.* have also the studied on the structural features and mechanical properties of PLLA/pearl powder scaffold. Pearl is also in the family of bivalve mollusk, the same family as *Lokan*. It also contain high amount of CaCO<sub>3</sub>.

From his study, it was also found that the porosity will change when Pearl powder filler is insert in the PLLA matrix. The number of pores as well as the pore size decreased, as the filler content increase. When porosity decrease, the Yield Strength will increase. From both studies, it can be seen that the addition of CaCO<sub>3</sub>, change the porosity of PLA matrix, hence improve the mechanical properties of the composite.

## CHAPTER 5

### CONCLUSION AND RECOMMENDATIONS

#### 5.1 Conclusion

For the characterization of the *Lokan* shell and *Lokan* powder as the source of biomineral, aragonite which is the valuable mineral polymorph was detected by using XRD analysis. The result was then confirmed with SEM where rod-like aragonite was observed and its elements were rich of oxygen and calcium without any detection of trace element (EDX).

For LP/PLA composite, based on the overall result, it can be seen that the addition of *Lokan* powder as filler to PLA matrix, peak intensity in XRD analysis, crystallinity, tensile properties, and porosity of the resulted composite has changed significantly.

From XRD analysis, 2 peaks are clearly shown for PLA/LP composite, which are the peak of PLA and the peak of aragonite. The intensity of PLA peak decreased with the increasing filler content and the intensity of aragonite peak increased with increasing filler content.

Meanwhile, for tensile analysis, it can be seen that the incorporation of LP improves the stiffness of the composite where there is an increase in Young's Modulus. For tensile strength of all sample, the value is varied slightly. There is no significant difference between the value of tensile strength, indicate that there is a good bonding between filler and particle, without any existence of debonding. However the addition of LP also loosens the ductility of the composite, thus only small amount of LP should be added to the composite to avoid early failure of the material.

In term of crystallinity, it can be concluded that the addition of LP decrease the crystallinity of PLA matrix, where 8wt% filler content, give the lowest degree of crystallinity among all sample. The degree of crystallinity is inversely proportional to the enthalphy of fusion. Thus, increasing the filler content will also decrease the enthalphy of fusion with lowest enthalphy also shown at 8wt% filler content. By looking at the onset temperature of crystallization, the additions of LP increase the onset temperature. This indicates that LP may play the role of nucleating agent. However, even though LP may play the role of nucleating agent, due to the limited movement of the PLA molecular chain will and the reduce of molecular chain, the enthalphy of fusion is decreased.

By looking at the FESEM analysis on the surface morphologies of all samples, poor distribution of particle can be seen in all composite samples and agglomeration of particle exist. This is due to the larger size of particle use as filler compared to other studies that has been done. When nanosize particle is used, the particle can be homogenously dispersed and agglomeration of particle

can be avoided. No debonding were found in all samples indicate that there is a good bonding between filler and matrix. Thus the there will be an effective load transfer between filler and matrix. In term of porosity of the composite, addition of LP filler, decrease significantly the amount of pores compared to neat PLA. Neat PLA is a highly porous structure, with large pore size and high amount of pores. When LP filler is added to PLA matrix, the pore is filled with  $\text{CaCO}_3$  particle, hence reducing the amount of pores. The pore size is also decrease where neat PLA have pore size is from 365nm -3.5 $\mu\text{m}$  and PLA/6wt% LP has pore size of 54.3nm-188.7nm. The decreased of amount of pores also lead to the increase of Young's Modulus of the material. Low porosity will leads to stiffer material. This support the result from tensile stress where Young's Modulus increase with the increase of filler content.

## 5.2 Recommendations

It is recommended to reduce the size of LP filler, to get uniform distribution of the particle in the sample. With good distribution of particle in the matrix, mechanical performance of the material can be further improved.

The bonding between filler and matrix may also be improved by doing surface treatment to *Lokan* powder. Silane may be used to coat the *Lokan* powder particle be to enhance the bonding between filler and matrix and prevent agglomeration.

Besides that mechanical stirrer should be used instead of magnetic stirrer. This is to ensure proper mixing and blending of LP particles and PLA matrix while increasing the homogeneity of the mixing.

The fracture mechanism of the composite should also be studied to make a comparison between the fracture mechanisms of the same composition of the composite that has been done by other researcher.

## CITED REFERENCE

- L. Xiang, Y. Xiang, Y. Wen, F. Wei. (2004) Formation of  $\text{CaCO}_3$  nanoparticles in the presence of terpineol, *Materials Letters*, 58, 959-965
- Ng, P. K., & Sivasothi, N. (2005) *Lokan (Polymesoda expansa)*. Retrieved September 18, 2009, from Guide To The Mangroves of Singapore: <http://mangrove.nus.edu.sg/guidebooks/text/2098.htm>
- Mona. R, (2008) Research Asia research News; Microwaving Waste Goodbye. Retrieved 20 June 2011 from <http://www.researchsea.com/html/article.php/aid/3264/cid/2>
- Hazmi, A. J., Zuki, A. B., Noordin, M., Jalila, A., & Norima, Y. (2007). Mineral Composition of the Cockle (*Anadara granosa*) Shells of West Coast of Peninsular Malaysia and It's Potential as Biomaterial for Use in Bone Repair. *Journal of Animal and Veterinary Advances* , 6 (5), 591-594.
- The European Calcium Carbonate Association. (2009). *Fact Sheet on Calcium Carbonate*. IMA Europe.
- M.G.A Vierra, M.A.D Silva, L.O.D Santos. (2011) Natural based plasticizers and biopolymer films: A review, *European Polymer Journal* ,47, 254-263
- R.N. Rothon. (2007) Paper I: The High Performance Fillers Market and The Position of Precipitated Calcium carbonate and Silica, *Proceedings of High Performance Filler* , Hamburg, Germany.
- F. Manoli, E. Dalas.(2000) Spontaneous precipitation of calcium carbonate in the presence of ethanol, isopropanol and diethylene glycol, *Journal of Crystal Growth*, 218, 359-364
- K. Nurul Islam, M. Z. Abu Bakar, M.E. Ali, M. Z. Hussein, M.M. Noordin, M.Y. Loqman, G. Miah, H. Wahid, U. Hashim. (2013) A novel method for the synthesis of calcium carbonate (aragonite) nanoparicles from cockle shells, *Powder Technology* , 235 , 70-75
- A. Lutts, J. Grandjean, C.Gregoire. (1960) X-ray diffraction patterns from the prisms of mollusc shells, *Achives of Physiology and Biochemistry* 68, 829-831
- W.J. Kennedy, J.D. Taylor, A. Hall. (1969) Environmental and biological controls on bivalve shell mineralogy, *Biological Reviews* 44, 499-530
- J.D. Taylor, W.J.Kennedy, A. Hall. (1969) The shell structure and mineralogy of the Bivalvia. Introduction., Nuculacea-Trigonacea, *Bulletin of the British Museum (Natural History) Zoology*, Supplement 3, 1-125
- B.Pokroy, J.S Fieramosca, R.B. von Dreele, A.N. Fitch, E.N. Caspi, E. Zolotoyabko. (2007) Atomic Structure of Biogenic Aragonite, *Chemistry of Materials* ,19, 3244-3251
- S.I. Stupp, P.V. Braun. (1997) Molecular manipulations of materials: biomaterials, ceramics and semiconductors, *Science*, 277, 1242

- I. Lee, S.W. Han, H.J. Choi, K. Kim. (2001) Nanoparticle-directed crystallization of calcium carbonate, *Advance Material*, 13, 1617–1620.
- H.Y. Ma, T.G. Dai. (2001) The first discovery of vaterite in lustreless freshwater pearls of Leidan, Zhejiang, *Acta Mineral Sin* , 21, 153-157
- J. Chen, L. Xiang. (2009) Controllable synthesis of calcium carbonate polymorphs at different temperatures, *Powder Technology*, 189, 64-69
- Z. Hu, Y. Deng. (2004) Synthesis of needle-like aragonite from calcium chloride and sparingly soluble magnesium carbonate, *Powder Technology* ,140 ,10-16
- FAO. (2011) National aquaculture sector overview: Malaysia. Food and Agriculture Organization, [http://www.fao.org/fishery/countrysector/naso\\_malaysia/en](http://www.fao.org/fishery/countrysector/naso_malaysia/en). (date: 15 Oct 2012)
- V. Do, P. Budha, B.A. Daniel. (2012) Polymesoda bengalensis. IUCN 2012. IUCN Red List of Threatened Species Version 2012.2 [www.iucnredlist.org](http://www.iucnredlist.org) (date: 21 Nov 2012)
- H. Hamli, M.H. Idris, M.K. Abu Hena, S.K. Wong S.K. (2012) Taxonomic Study of Edible Bivalve from Selected Division of Sarawak, Malaysia. *International Journal of Zoological Research* ,8, 52-58.
- Poutiers, M. (1998) The Living Marine Resources of the Western Central Pacific. In: FAO Species Identification Guide for Fishery Purpose, K.E. and V.H. Niem (Eds.). *Food and Agriculture Organization of the United Nations, Rome, Italy*, Vol. 1 , pp: 363-386
- N.A Mohamad Yusoff, N.A. and Mohd Long. (2011) Preliminary study on the accumulation of heavy metal concentration in edible mollusk from Sungai Sematan estuary, *Research Bulletin Faculty of Resource Science and Technology Universiti Malaysia Sarawak*, Vol. 1, 5-6
- S. Nakao, H. Nomura and M.K.B.A. Satar. (1989) Macrobenthos and Sedimentary Environments in a Malaysian Intertidal Mudflat of the Cockle bed. *Buletin Faculty of Fishery Science Hokkaido Univ* ,40 , 203-213.
- Ong, C.C., K. Yusoff, C.K. Yap and S.G. Tan. (2009) Genetic characterization of *Perna viridis* L. in peninsular Malaysia using microsatellite markers. *Genetika* 88 153-163.
- B.Y. Kamaruzzaman, M.S. Zahir, B. Akbar John, A. Siti Waznah, K.C.A. Jalal, S. Shahbudin, S.M. Al-Barwani and J.S. Goddard. (2010) Determination of Some Heavy Metal Concentrations in Razor Clam (*Solen brevis*) from Tanjung Lumpur Coastal Waters, Pahang, Malaysia. *Pakistan Journal of Biological Sciences*, 13, 1208-1213.
- D. Kanakaraju, F Ibrahim, M.N Berseli. (2008) Comparative study of heavy metal concentrations in razor clam (*Solen regularis*) in Moyan and Serpan, Sarawak, *Global Journal of Environmental Research* ,2.2 ,87-91.

- R. Auras, B. Harte, and S. Selke. 2004. "An Overview of Polylactides as Packaging Materials," *Macromolecular Bioscience*, vol. 4, pp. 835-864.
- J. Lunt. 1998. "Large-scale production, properties and commercial applications of polylactic acid polymers," *Polymer Degradation and Stability*, vol. 59, pp. 145-152.
- M. Vert, G. Schwarch, and J. Coudane. (1995) "Present and Future of PLA Polymers," *Journal of macromolecular science. Part A, Pure & applied chemistry*, vol. A32, pp. 787-796.
- R. E. Drumright, P. R. Gruber, and D. E. Henton. (2000) "Polylactic Acid Technology," *Advanced Materials*, vol. 12, pp. 1841-1846
- S. Mecking. (2004) "Nature or Petrochemistry? - Biologically Degradable Materials," *Angewandte Chemie International Edition*, vol. 43, pp. 1078-1085.
- Y. Ikada and H. Tsuji. (2000) "Biodegradable polyesters for medical and ecological applications," *Macromolecular Rapid Communications*, vol. 21, pp. 117-132,.
- D. Cam and M. Marucci. (1997) "Influence of residual monomers and metals on poly (-lactide) thermal stability," *Polymer*, vol. 38, pp. 1879-1884.
- A. Celli and M. Scandola. (1992) "Thermal properties and physical ageing of poly (-lactic acid)," *Polymer*, vol. 33, pp. 2699-2703.
- G. Perego, G. Domenico, and C. C. Bastioli. (1996) "Effect of molecular weight and crystallinity on poly(lactic acid) mechanical properties," *Journal of Applied Polymer Science*, vol. 59, pp. 37-43.
- T.D Lam, T.V Hoang, D.T Quang and J.S Kim. (2009) "Effect of nanosized and surface modified precipitated calcium carbonate on properties of CaCO<sub>3</sub>/polypropylene nanocomposites," *Materials Science and Engineering*, Vol. A 501, pp. 87-93.
- L.Jiang, J.Zhang and M.P Wolcott. (2007) "Comparison of polylactide/nanosized calcium carbonate and polylactide/montmorillonite composites: Reinforcing effect and toughening mechanisms," *Polymer*, Vol. 48, pp. 7362-7644.
- M.G.A.Vieira, M.A.D. Silva, L.O.D Santos and M.M Beppu. (2011) " Natural Base Plasticizers and biopolymer film: A review ," *European Polymer Journal*, Vol. 47, pp. 254-263,

## APPENDICES

- 1) Figure A1. Reference pattern of aragonite
- 2) Figure A2. Reference pattern of pure PLA
- 3) Figure A3. Neat PLA, stress-strain curve
- 4) Figure A4 PLA/2wt%LP , stress strain curve
- 5) Figure A5 PLA/4wt%LP , stress strain curve
- 6) Figure A6 PLA/6wt%LP , stress strain curve
- 7) Figure A7 PLA/8wt%LP , stress strain curve
- 8) Figure A8 PLA/10wt%LP , stress strain curve
- 9) Figure A9 Fracture image for neat PLA
- 10) Figure A10 Fracture image for PLA/2wt% LP
- 11) Figure A11 Fracture image for PLA/4wt% LP
- 12) Figure A12 Fracture image for PLA/6wt% LP
- 13) Figure A13 Fracture image for PLA/8wt% LP
- 14) Figure A14 Fracture image for PLA/10wt% LP
- 15) Figure A15 DSC curve for neat PLA
- 16) Figure A16 DSC curve for PLA/2wt% LP
- 17) Figure A17 DSC curve for PLA/4wt% LP
- 18) Figure A18 DSC curve for PLA/6wt% LP
- 19) Figure A19 DSC curve for PLA/8wt% LP
- 20) Figure A20 DSC curve for PLA/10wt% LP

### **Name and formula**

Reference code: 00-041-1475

Mineral name: Aragonite

Compound name: Calcium Carbonate

Empirical formula:  $\text{CCaO}_3$

Chemical formula:  $\text{CaCO}_3$

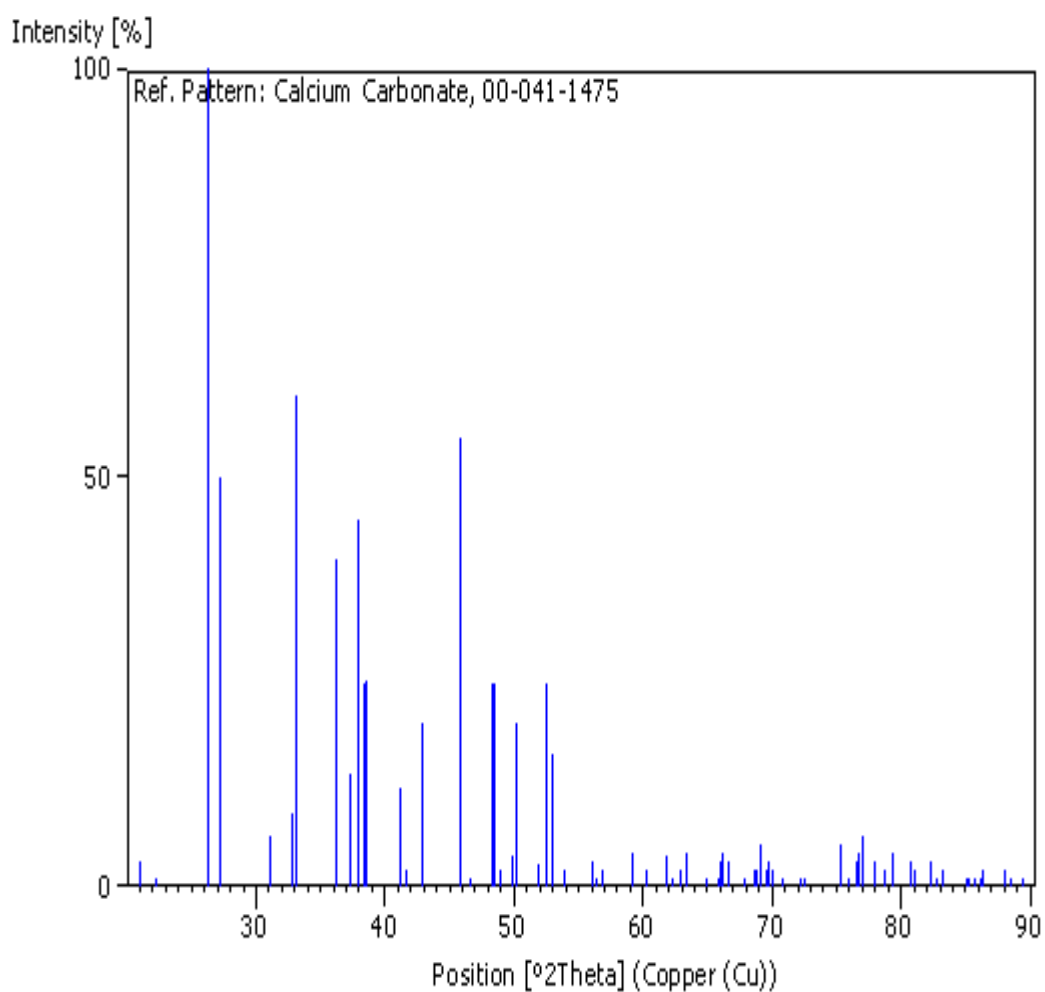


Figure A1 Reference pattern of aragonite Calcium Carbonate

**Name and formula**

Reference code: 00-054-1917

Compound name:  $\alpha$ -Poly(D-lactide)

Empirical formula:  $C_3H_5O_3$

Chemical formula:  $(C_3H_5O_3)_n$

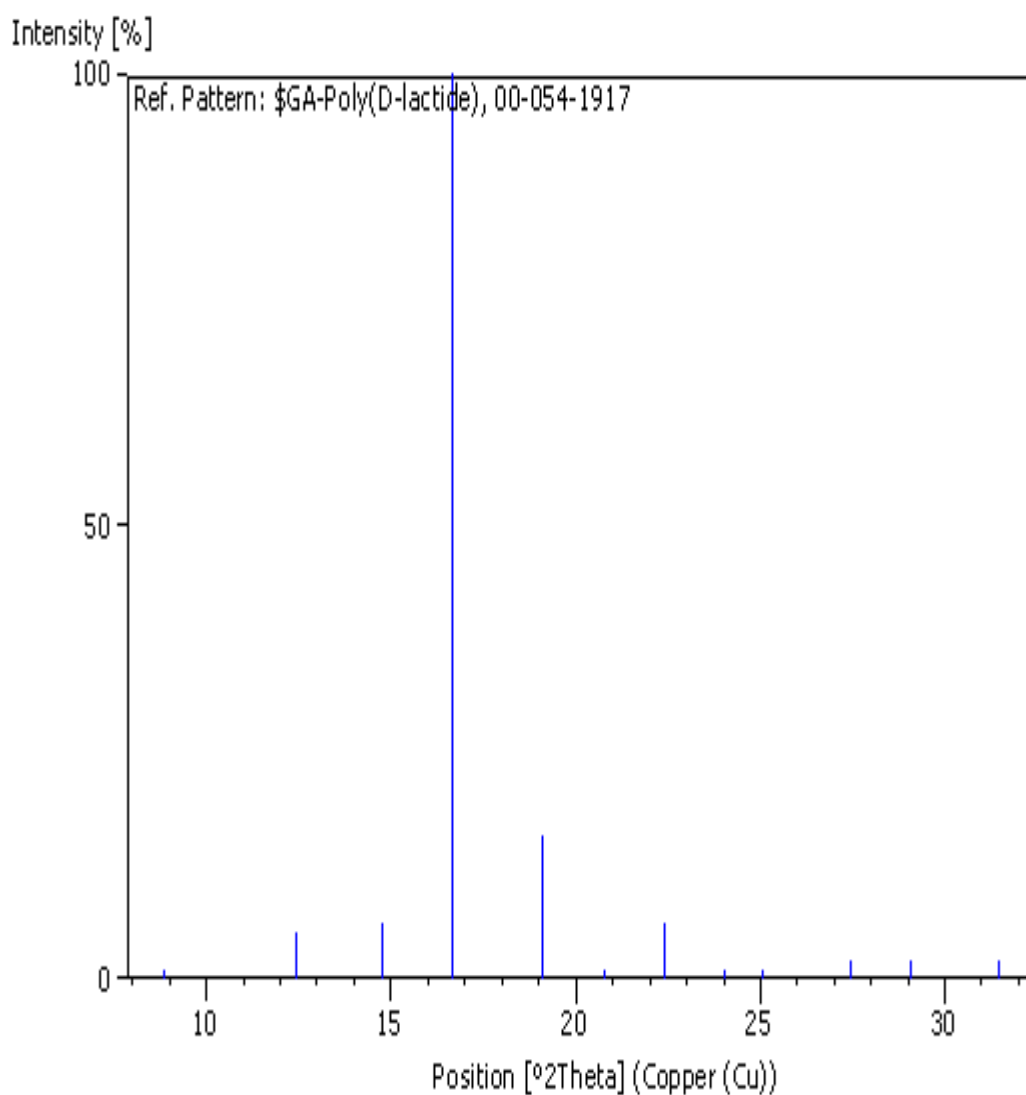


Figure A2 Reference pattern of PLA

Sample ID: 0E

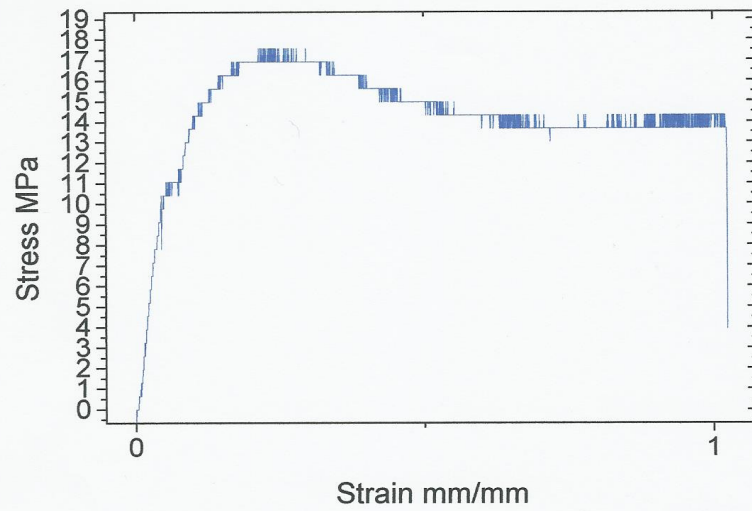


Figure A3 Stress strain curve of neat PLA

Sample ID: E2

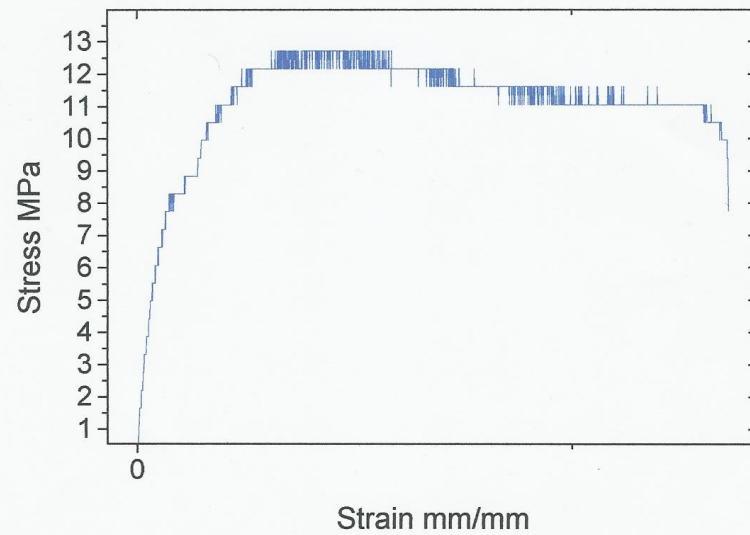


Figure A4 Stress strain curve PLA/2wt% LP

Sample ID: A4

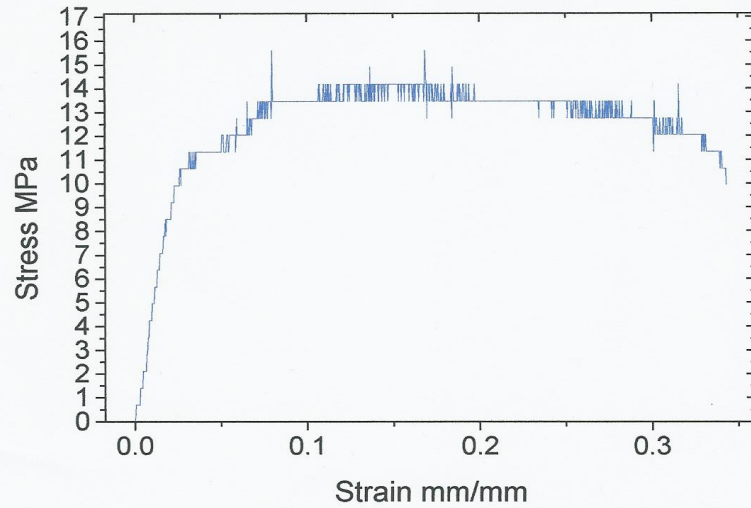


Figure A5 Stress strain curve PLA/4wt% LP

Sample ID: C6

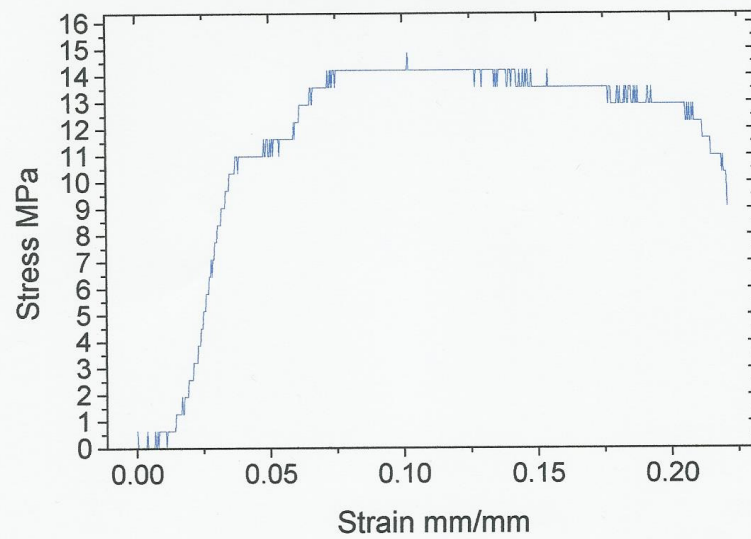


Figure A6 Stress strain curve PLA/6wt% LP

Sample ID: 8B

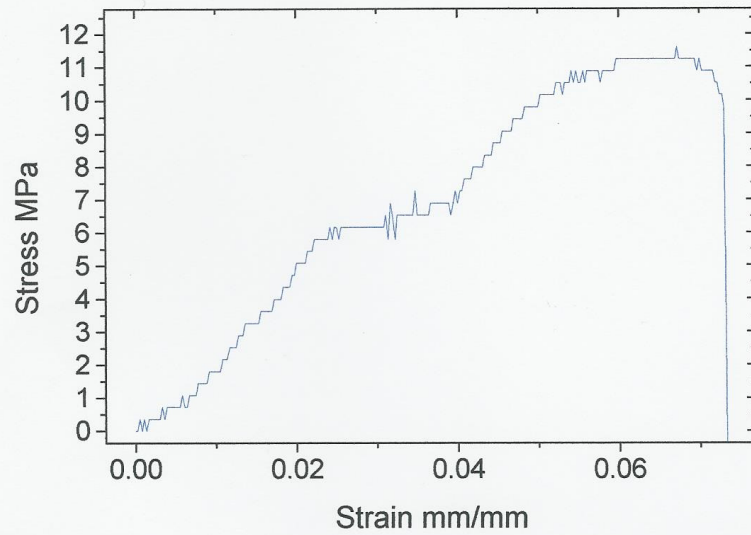


Figure A7 Stress strain curve PLA/4wt% LP

Sample ID: 10C

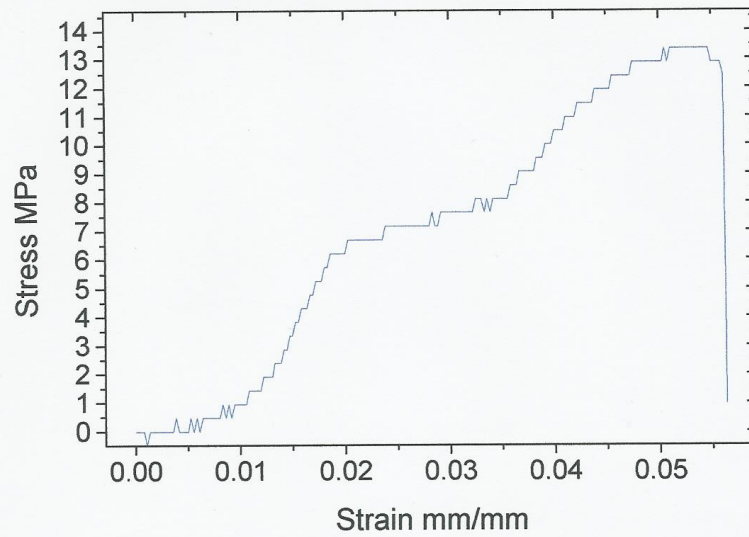


Figure A8 Stress strain curve PLA/10wt% LP



Figure A9 Fracture image of neat PLA

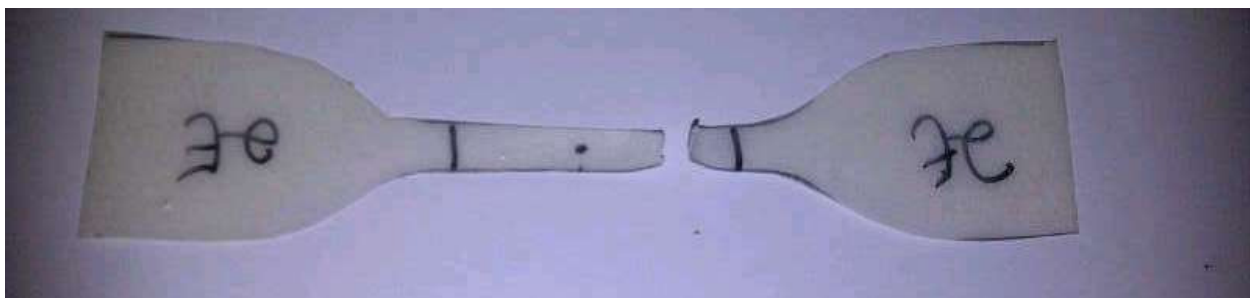


Figure A10 Fracture image of PLA/2wt% LP



Figure A11 Fracture image of PLA/4wt% LP



Figure A12 Fracture image of PLA/6wt% LP

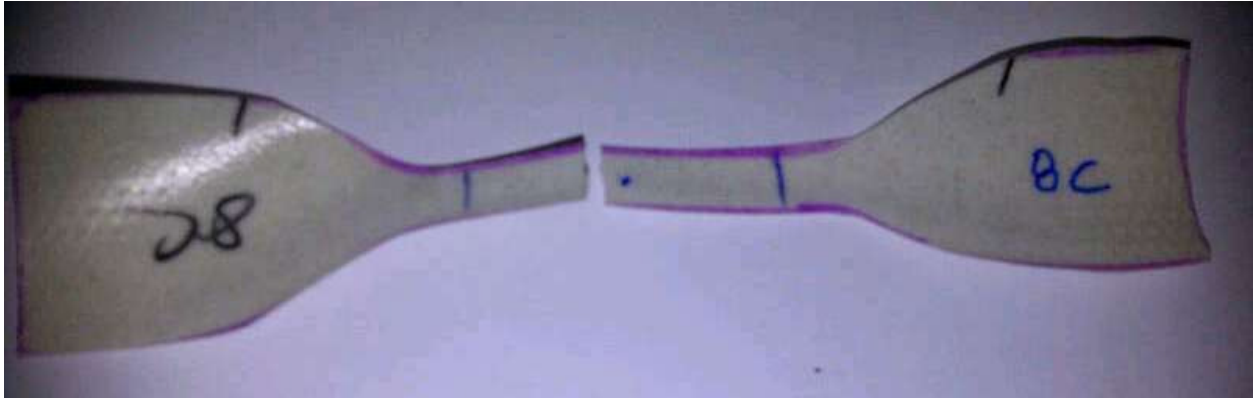


Figure A13 Fracture image of PLA/8wt% LP

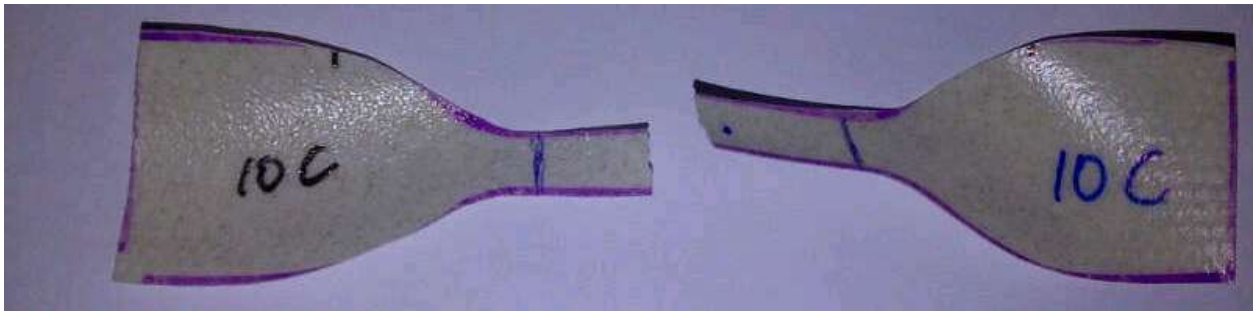


Figure A14 Fracture image of PLA/10wt% LP

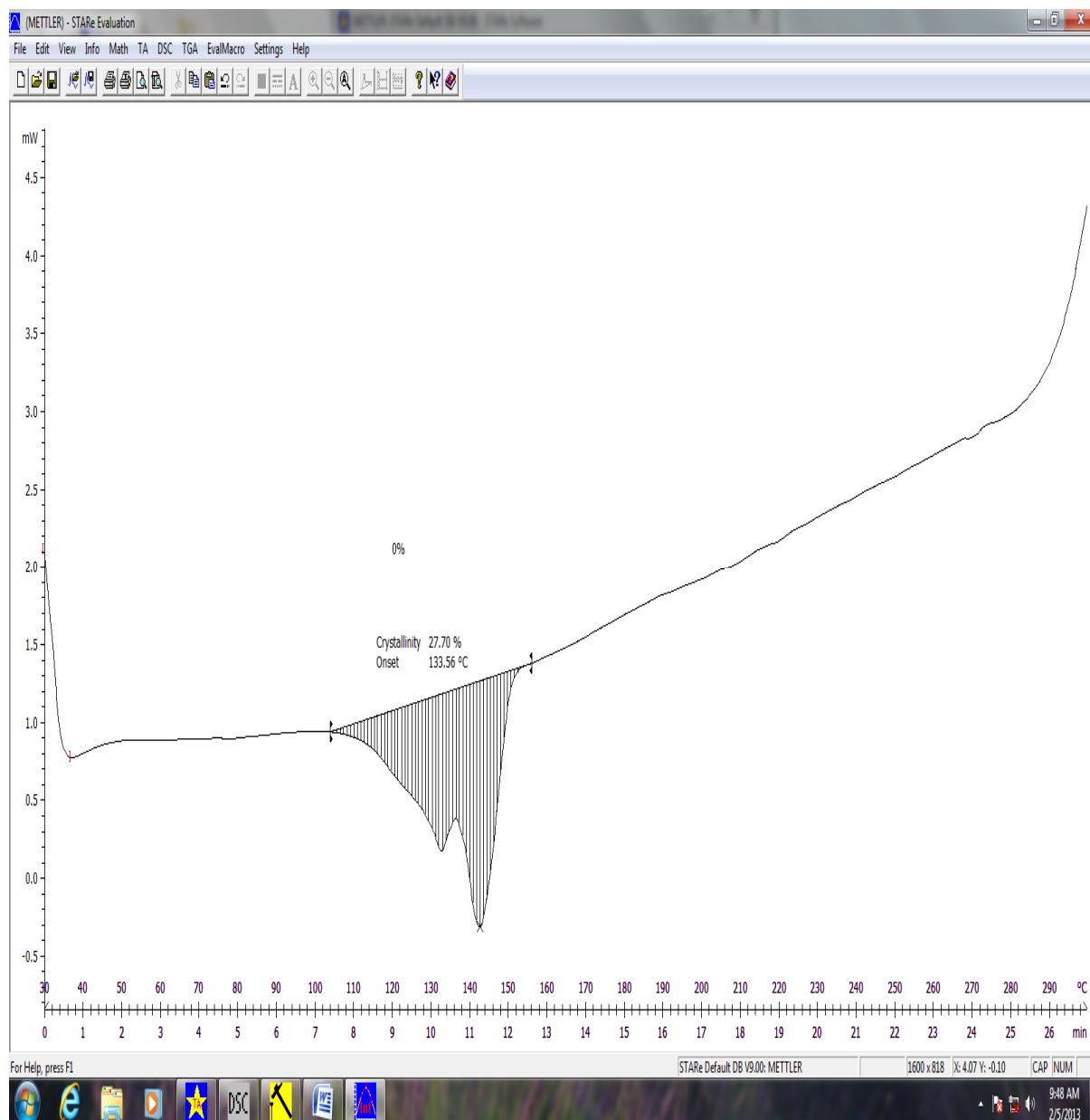


Figure A15 DSC curve of neat PLA

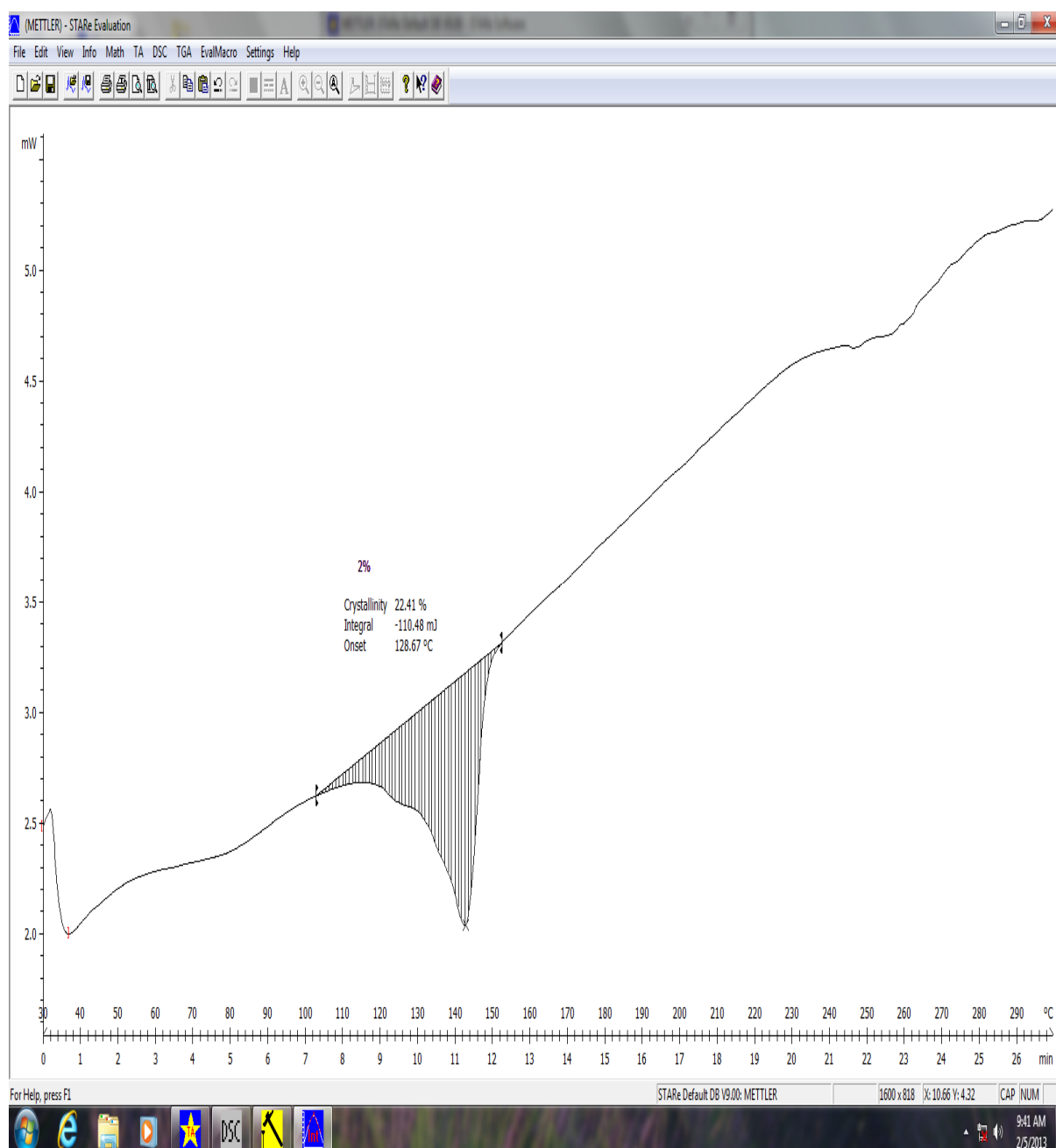


Figure A16 DSC curve of PLA/2wt% LP

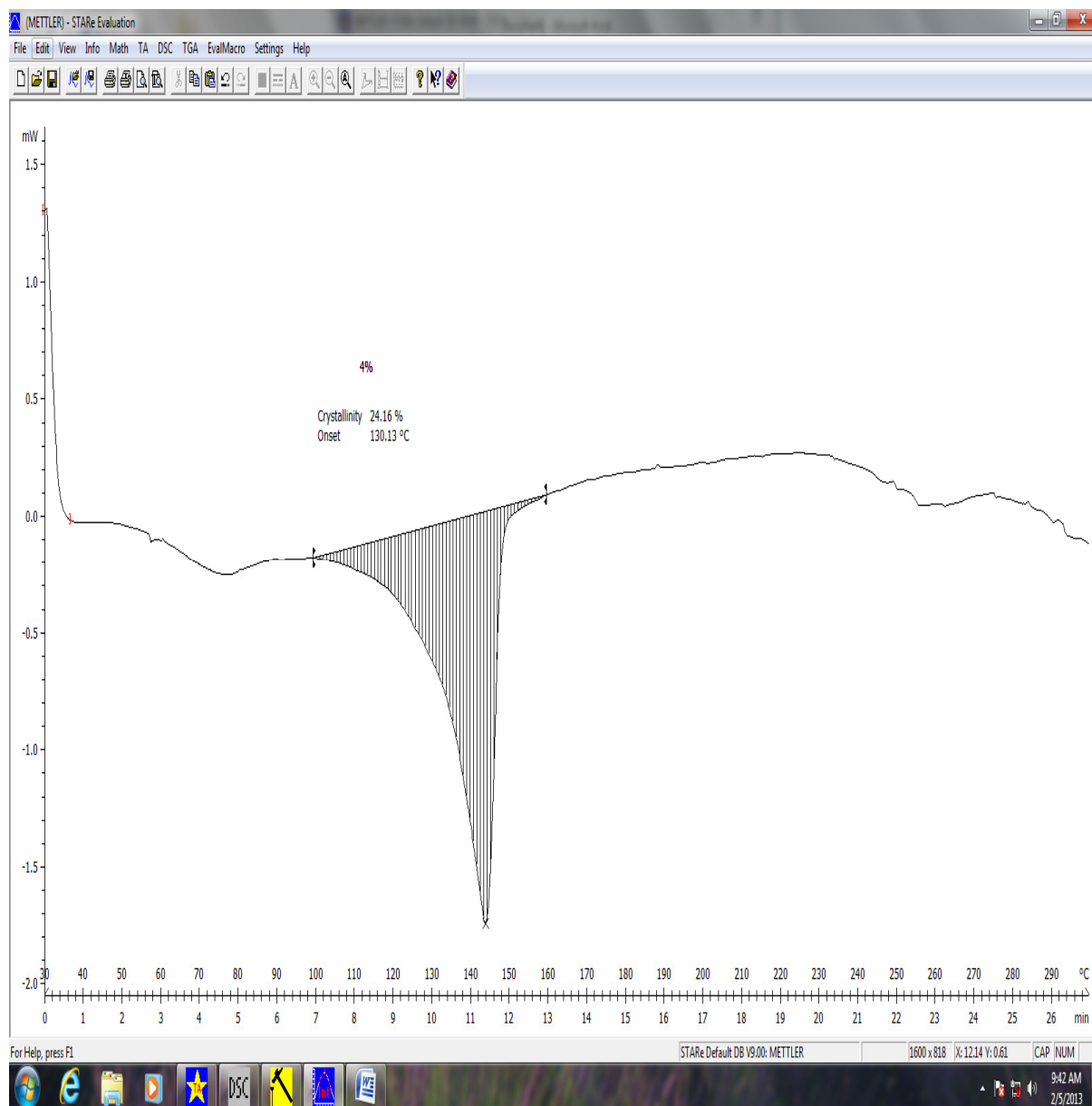


Figure A17 DSC curve of PLA/4wt% LP

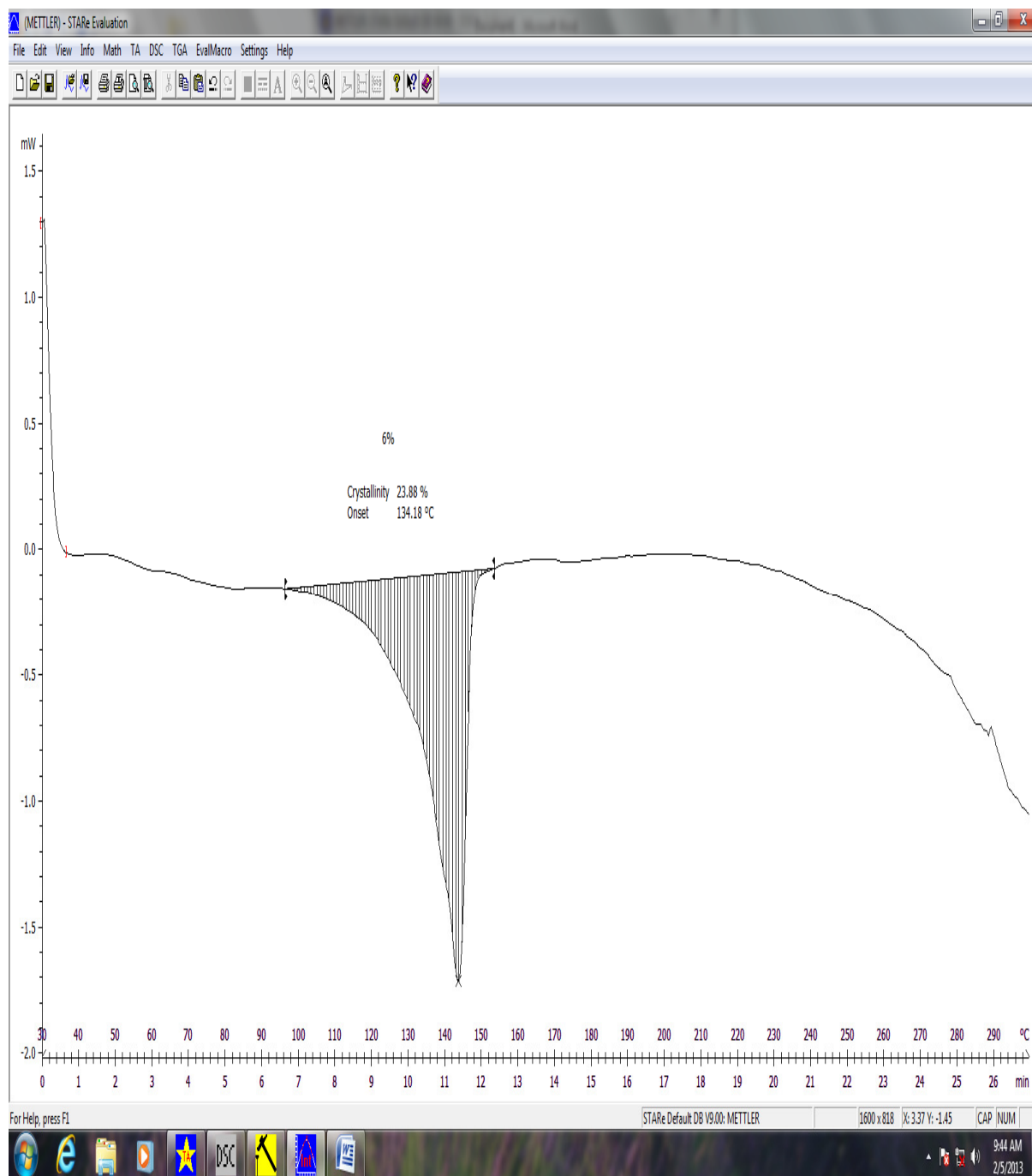


Figure A18 DSC curve of PLA/6wt% LP

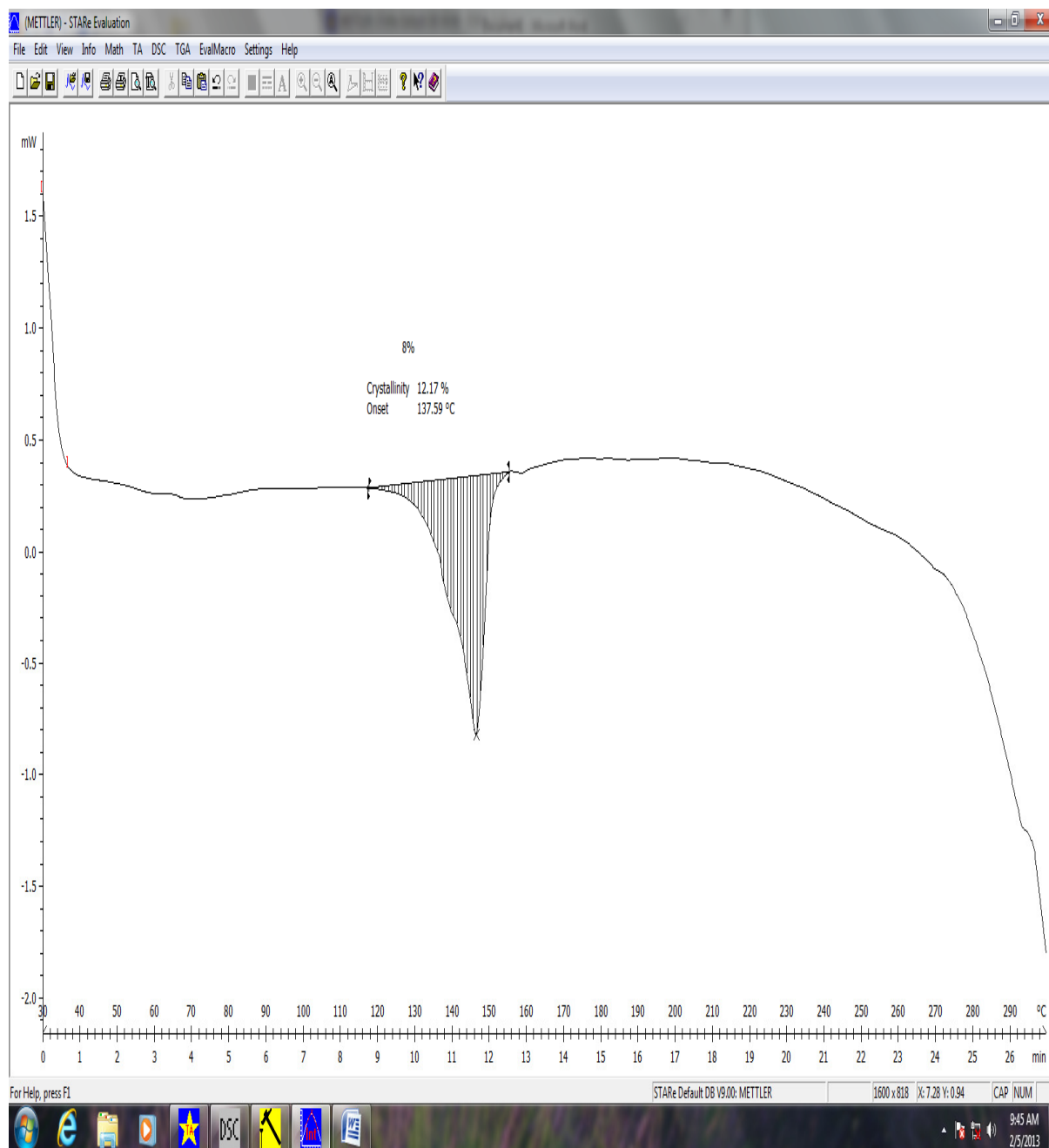


Figure A19 DSC curve of PLA/8wt% LP

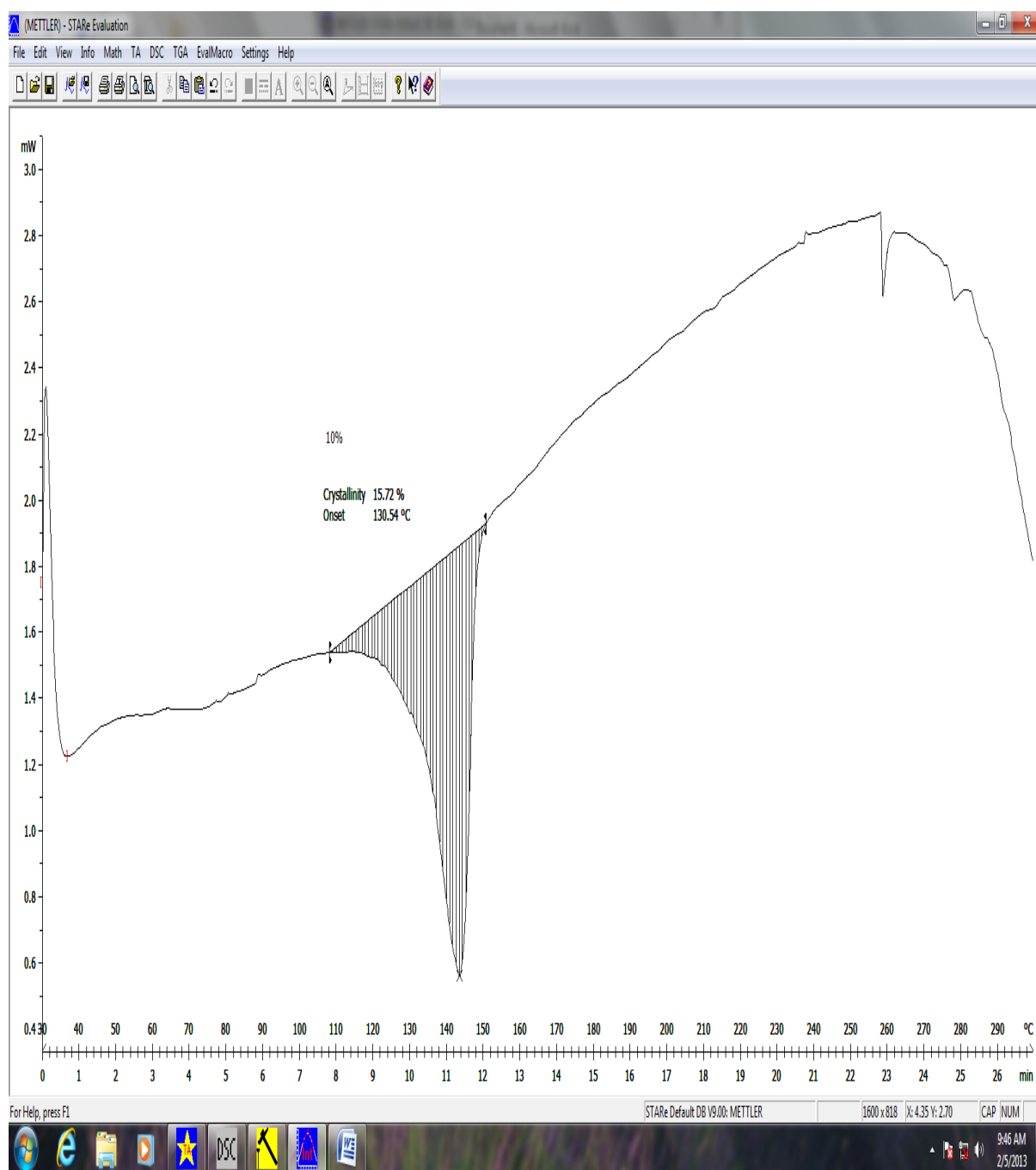


Figure A20 DSC curve of PLA/10wt% LP